Class I Histone Deacetylases in Retinal Progenitors and Differentiating Ganglion Cells

[#]Ankita Saha[1, 2,] [#]Sarika Tiwari[1, 2], Subramanian Dharmarajan[1, 2], *Deborah C. Otteson[3], and *Teri L. Belecky-Adams[1, 2]

*Both of the authors are corresponding authors

[#]These authors contributed equally to this work

[1]Department of Biology, Indiana University-Purdue University Indianapolis, 723 W Michigan St, Indianapolis, IN-46202. [2]Center for Developmental and Regenerative Biology, Indiana University- Purdue University Indianapolis, 723 W Michigan St, Indianapolis, IN-46202. [3] University of Houston College of Optometry, 4901 Calhoun Rd. Rm 2195, Houston, TX 77204-2020.

Ankita Saha:ankitasaha2221@gmail.com

Sarika Tiwari: sjtiwari@gmail.com

Subramanian Dharmarajan: sdharmar@umail.iu.edu

Keywords: Histone Deacetylases, HDACs, mouse, murine, retina, progenitors, retinal ganglion cells

Running Title: HDAC Localization in Murine Retina

Correspondence should be sent to the following addresses:

Teri L Belecky-Adams
Department of Biology, SL306
Center for Developmental and Regenerative Biology
Indiana University-Purdue University Indianapolis.
723 W Michigan St.
Indianapolis, IN-46202
Tel. (317)278-5715
Fax (317) 274-2846
E-mail: tbadams@iupui.edu

This is the author's manuscript of the article published in final edited form as:

Saha, A., Tiwari, S., Dharmarajan, S., Otteson, D. C., & Belecky-Adams, T. L. (2018). Class I histone deacetylases in retinal progenitors and differentiating ganglion cells. Gene Expression Patterns. https://doi.org/10.1016/j.gep.2018.08.007

Deborah C. Otteson
University Eye Institute, Room 2195
University of Houston
4901 Calhoun Rd.
Houston, TX 77204-2020
Tel. (713) 743-1952
Fax (713) 74302053
E-mail: dotteson@central.uh.edu

Abstract

Background: The acetylation state of histones has been used as an indicator of the developmental state of progenitor and differentiating cells. The goal of this study was to determine the nuclear localization patterns of Class I histone deacetylases (HDACs) in retinal progenitor cells (RPCs) and retinal ganglion cells (RGCs), as the first step in understanding their potential importance in cell fate determination within the murine retina. **Results:** The only HDAC to label RPC nuclei at E16 and P5 was HDAC1. In contrast, there was generally increased nuclear localization of all Class I HDACs in differentiating RGCs. Between P5 and P30, SOX2 expression becomes restricted to Müller glial, cholinergic amacrine cells, and retinal astrocytes. Cholinergic amacrine showed a combination of changes in nuclear localization of Class I HDACs. Strikingly, although Müller glia and retinal astrocytes, express many of the same genes, P30 Müller glial cells showed nuclear localization only of HDAC1, while retinal astrocytes were positive for HDACs 1, 2, and 3. **Conclusion:** These results indicate there may be a role for one or more of the Class I HDACs in retinal cell type-specific differentiation.

1. Introduction

The retina is a highly ordered neural tissue that converts light into neural signals, which are transmitted to the brain where they are interpreted as vision. Throughout retinal development, the timing and patterns of cellular differentiation are regulated, in part, by the hierarchical expression of various gene regulatory networks. Combinatorial expression of eyefield transcription factors, including PAX6, RAX, SIX6, and LHX2, demarcate the eye field within the anterior neural plate, thereby conferring the competence for formation of ocular structures (Tetreault et al., 2009; Zuber et al., 2003). During embryogenesis, multipotent retinal progenitors within the retinal neuroepithelium undergo progressive restriction in their competence to generate the seven basic cell types of the mature retina: rod and cone photoreceptors, amacrine, bipolar, horizontal and retinal ganglion cells, and Müller glia (Wong and Rapaport, 2009). PAX6 is an early competence factor that appears to be important the generation of all retinal cell types (with the exception of amacrine cells) that functions upstream of bHLH factor ATOH7 (Brown et al., 2001; Brzezinski et al., 2005; Marquardt et al., 2001; Wang et al., 2001). Competence for early born cell types, such as cone photoreceptors, horizontal, and retinal ganglion cells, is thought to be conferred by the zinc finger transcription factor IKAROS, whereas late born cell types appear to require activity of DICER to process micro RNAs that are critical for differentiation of rods, bipolar cells, and Müller glia (Elliott et al., 2008; Georgi and Reh, 2010; Iida et al., 2011; La Torre et al., 2013).

Differentiation of progenitors into the different types of retinal neurons and Müller glia occurs in a sequential, but temporally overlapping pattern and requires expression of various transcription factors such as selective Sry-related high mobility group box (SOX) factors and proneural basic helix-loop-helix (bHLH) factors, which function as competence factors (Graw, 2010; Hufnagel et al., 2010; Jiang et al., 2013; Mu et al., 2005; Phillips et al., 2014; Riesenberg et al., 2009; Taranova et al., 2006; Yang et al., 2003; Young, 1985). Mice in which *Sox4* and *Sox11* were both knocked out showed a loss of retinal ganglion cells and a decrease in the expression of later differentiation factor BRN3b expression (Jiang et al., 2013). SOX2 and 11 appear to operate independently of bHLH factors in that knock out animals showed normal *Atoh7* expression levels. SOX2 has also been proposed as a competence factor, however it seems to act more as a general competence factor for retinal progenitor cells (Elliott et al., 2008; Taranova et al., 2006). Expression of several bHLH genes has also been shown to confer competence on retinal ganglion cells, primarily *Atoh7* (Brzezinski et al., 2012; Maurer et al., 2014; Mu et al., 2008; Mu et al., 2005), *NeuroD1* (Kiyama et al., 2011; Mao et al., 2008b) and *Ngn2* (Matter-Sadzinski et al., 2005). These bHLH transcription factors regulate the earliest of

RGC-specific transcription factors, POU4F1-3 (BRN3A-C) and other RGC-specific genes that are critical for differentiation, defining RGC subpopulations, and ultimately, RGC connectivity and function (Gan et al., 1996; Mao et al., 2008a; Matter-Sadzinski et al., 2005; Mu et al., 2008).

There have been significant advances in understanding the roles of the transcriptional regulatory networks and signaling pathways in retinal development and the establishment of competence. However, other factors, such as chromatin organization, also play critical roles in both competence restriction of progenitor cells and differentiation of cells from the progenitor population (Cvekl and Mitton, 2010; Eberhart et al., 2013; Schmalenberger, 1980; Solovei et al., 2009; Song et al., 2014; Van Bortle and Corces, 2013). At the most basic level, chromatin is organized into transcriptionally active euchromatin and inactive heterochromatin (Solovei et al., 2016). This organization can be modified by changes in methylation patterns within genomic CpG islands and/or by post-translational modifications of histone core and tail domains (Mersfelder and Parthun, 2006). To date, the best studied examples of these histone modifications are acetylation, methylation, phosphorylation, and ubiquitination (Rousseaux and Khochbin, 2015). Although a case can be made for differential effects of site-dependent acetylation in chromatin regulation, increased histone acetylation is generally associated with gene activation (Haberland et al., 2009).

Histone acetylation is regulated by two families of enzymes with antagonistic roles: histone acetyl transferases (HATs) add acetyl groups to specific lysine residues, whereas histone deacetylases (HDACs) are responsible for their removal (Chen et al., 2015). HDACs are subdivided into the zinc-dependent classical HDACs (HDACs 1-11) and NAD+ dependent sirtuins (SIRT1-7). These two groups are further subdivided into four classes based on molecular similarities with yeast homologues (Gregoretti et al., 2004). The zinc-dependent classical HDACs constitute Classes I, II, and IV deacetylases, while the NAD^+ dependent sirtuins constitute the Class III deacetylases (Delcuve et al., 2013). Class I HDACs, including HDACs 1, 2, 3 and 8, show predominantly, although not exclusively, nuclear localization, whereas Class II HDACs, including HDACs 4-7, 9, and 10, shuttle between the nucleus and cytoplasm (Kong et al., 2011). The Class IV HDAC is comprised solely of HDAC 11 and appears to be predominantly nuclear (Gao et al., 2002).

Histone modifications play a key role in regulating chromatin organization and gene expression, and have been implicated in modulating the transition from proliferation to differentiation in neuronal cells (reviewed by (Jaworska et al., 2015; Reichert et al., 2012)). However, little is known about the role of specific HDACs during retinal development. Class I HDACs are of

particular interest because they regulate gene expression via recruitment to repressor protein complexes within the nucleus, including SIN3, spermatogenic HDAC-interacting protein 1 (SHIP1), nuclear receptor corepressor (NCoR), silencing mediator for retinoid and thyroid receptors (SMRT), nucleosome remodeling deacetylase (NuRD), and RE1-silencing transcription factor (REST) complexes (Thomas, 2014).

There is evidence supporting a critical role of HDACs in regulating differentiation of progenitors in the central nervous system (CNS). HDAC1 is involved in multiple processes during neurogenesis, including suppression of cell cycle exit, inhibition of WNT and notch signaling, regulation of developmental apoptosis and positive regulation of neurogenic genes (Harrison et al., 2011; Stadler et al., 2005; Yamaguchi et al., 2005). Trichostatin A inhibition of HDAC activity in the neonatal mouse retina increases the extent of normal developmental apoptosis (Wallace et al., 2006), and shRNA downregulation of HDAC4 in the postnatal retina results in apoptosis of newly differentiated rod photoreceptors and bipolar cells (Chen and Cepko, 2009). Although HDACs regulate histone acetylation at a global level within cells, there is some evidence for a role in regulating sets of specific genes (Chen and Cepko, 2007; Haberland et al., 2009). A potential role for HDACs in regulating cell type-specific programming is suggested by the fact that the specificity of each HDAC is dependent upon the binding partners present in the cell. The roles of HDACs in the developing mammalian retina have not been fully elucidated. Research has primarily focused on the role of these proteins in retinal and CNS diseases. As a first step to delineating the role of this critical family of enzymes in retinal development, we determined the temporal and cellular expression patterns of Class I HDACs in the developing murine retina in retinal progenitor cells and differentiating RGCs.

2. Results

2.1 Acetylated and methylated histone H3 expression in the developing murine retina

Post-translational modifications of histones have been correlated with relative accessibility of chromatin to transcription factors and RNA polymerase complexes. Histone H3 can be either acetylated or methylated at lysine 9, with the levels of acetylation vs. methylation respectively serving as good predictors of underlying promoter activation vs. silencing (Du et al., 2015; Karmodiya et al., 2012). The cellular distribution of acetylated histone H3 at lysine 9 (H3K9ac), as a marker of an open chromatin state, and of tri-methylated histone H3 at lysine 9 (H3K9me3), as a marker of a closed chromatin state (Bannister and Kouzarides, 2011) was analyzed by immunostaining across retinal development. Three developmental stages were chosen for the study: embryonic day 16 (E16) to represent the early proliferative state of the retina, when the retina consists primarily of progenitor cells and early born ganglion and cone cells; postnatal day 5 (P5), when the retina contains multiple classes of differentiated neurons and late stage proliferating progenitors; and postnatal day 30 (P30), when the retina is fully differentiated and no progenitors remain (Young, 1985). In addition to labeling with antibodies specific for each Class I HDAC, control sections at each stage were also incubated with isotypic IgG in place of the primary antibody (Supplementary Fig 1), as well as with no primary antibody.

At E16, a subset of nuclei at the scleral edge of the retinal neuroepithelium (Fig 1A: arrows) and in the nascent nerve fiber layer (Fig1A: arrowheads) were H3K9ac+. In contrast, H3K9me3 immunopositive cells were detected throughout the retina (Fig 1B). Cells that were immuno-positive for the H3K9ac modification were also co-labeled with the H3K9me3 (Fig 1A-C: arrows and arrowheads). At P5, H3K9ac was detected in fewer cells, compared to E16, and the majority of labeled cells located at the sclerad margin of the retina (Fig 1D). Similar to E16, H3K9me3 immunoreactivity continued to be detected in nuclei of essentially all retinal cells, and again, cells positive for H3K9ac were co-labeled for H3K9me3 (Fig 1D-F). At P30, the H3K9ac modification was not detected within the retina (Fig 1G). In contrast, H3K9me3 was detected in nuclei throughout the retina, although the intensity of staining appeared to be reduced compared to E16 and P5 (Fig 1H, I).

2.2 Quantitation of Hdac mRNA and protein in developing murine retina

To further explore the basis for the dynamic patterns of histone acetylation throughout retinal development, levels of Class I *Hdacs* were investigated by RT-qPCR (Fig 2A) and western blot

(Fig 2B). *Hdac1* showed a small increase in mRNA expression at P5 in comparison to E16, and a subsequent decrease at P30. *Hdac2* (Fig 2A) expression progressively decreased during development, with levels subsequently reduced by 73% at P30 (p=0.001 vs. E16). *Hdacs 3* and *8* levels showed little change across the timepoints examined (Fig 2A). However, apparent differences in *Hdac1, Hdac3 and Hdac8* mRNA expression did not reach statistical significance.

Antibodies against the Class I HDACs labeled a single band at the predicted molecular weights in whole retinal lysates, confirming specificity of the antibodies in western blotting (Fig 2B). At E16, P5 and P30, there were subtle changes in the intensity of the bands that for HDAC1 and HDAC2 that followed the general patterns of their transcript levels. HDAC8 protein levels appeared to decrease at P30, in comparison to E16 and P5, despite the absence of detectible changes in mRNA expression. However, after normalization to β-tubulin controls, none of the apparent changes in protein band intensity reached statistical significance.

2.3 Localization of HDACs in differentiating Retinal Ganglion, Cholinergic Amacrine, and Retinal Astrocytes in the Developing Murine Retina

Although overall protein levels did not change considerably throughout retinal development, we hypothesized that changes in nuclear HDAC localization could be associated with differentiation of specific cell types. To test this idea, comparative analyses were done to determine nuclear co-localization of Class I HDACs (HDACs 1, 2, 3, and 8) with (1) a nuclear marker for retinal progenitor cells (SOX2) at E16 and P5, (2) a nuclear marker of retinal ganglion cells (RGCs) (POU4F1 or 3) at E16, P5 and P30, and (3), Müller glial cells, retinal astrocytes, and a subset of cholinergic amacrine cells (SOX2) at P5 and P30 (Tables I and II; Figs 3-6).

2.3a HDAC1

Early stage retinal progenitors at E16 showed nuclear co-localization of SOX2 and HDAC1 (Fig 3A; Supplementary Fig 2A, B). In contrast, late stage SOX2+ retinal progenitor nuclei at P5 were predominantly negative for HDAC1 (Fig 3C; open arrows). An interesting pattern of HDAC1 labeling was detected at P5 in a subpopulation of cells at the outer edge of retina (Fig 3C, D). While we did not co-label these cells for cell type-specific markers, the pattern is similar to that observed by other investigators in GABA+ horizontal cells in the developing mouse retina (Schubert et al., 2010). At P30, HDAC1 labeled nuclei were present throughout the retina, and

included the SOX2+ Müller glia (Fig 3E; open arrows), cholinergic amacrine cells (Fig 5E: closed arrows) and retinal astrocytes (Fig 5E: arrowheads).

RGCs are one of the first class of neurons generated during retinal development and they begin to express POU4F transcription factors shortly after exiting cell cycle (Pan et al., 2005). At E16, all POU4F+ retinal ganglion cell nuclei were double-labeled for HDAC1, with migrating RGCs within the neuroblastic layer, showing less intense labeling than differentiated RGCs in the ganglion cell layer (Fig 3B; Supplementary Fig 2C, D: arrows). Mature RGCs continued to have robust nuclear staining for HDAC1 at P5 (Fig 3D) and P30 (Fig 3F).

SOX2+ cholinergic amacrine cells (Fig 3C, E: closed arrows) and retinal astrocytes (Fig 3C, E: arrowheads) showed co-localization of SOX2 and HDAC1 at both P5 and P30. SOX2+ Müller glia also showed HDAC1 nuclear co-localization at P30 (Fig. 3: open arrows). At P5 and P30, additional HDAC1 positive/SOX2 negative nuclei were present in the inner nuclear layer and likely included additional subtypes of amacrine cells and bipolar cells but were not specifically identified using cell type-specific markers in this study. Sections treated with preabsorbed antibody (Fig 3G-I) or IgG (Supplementary Fig 1) showed no HDAC label at any of the stages examined.

2.3b HDAC2

Compared to HDAC1, the cellular localization of HDAC2 (Fig. 4) was more variable across retinal development, with generally diffuse, punctate staining at E16, robust nuclear staining in differentiated neurons in the inner nuclear and ganglion cell layers at P5 and P30. At both E16 and P5, nuclei of retinal progenitors had little or no colocalization of HDAC2 with SOX2 (Fig. 4A, C: open arrows).

At E16, migrating RGCs in the neuroblastic layer also lacked nuclear HDAC2 staining (Fig. 4B: open arrows). There was some co-localization of HDAC2 and POU4F immunostaining in RGC nuclei in the ganglion cell layer at E16 (Fig. 4B: arrows) that was robust by P5 (Fig. 4D) and P30 (Fig 4F).

Some of the HDAC2+ nuclei in the ganglion cell layer were identified as presumptive retinal astrocytes, based on co-localization with SOX2 at E16, P5 and P30 (Fig. 4A, C, E: arrowheads). SOX2+ cholinergic amacrine cells were also HDAC2+ at P5 and P30 (Fig. 4C, E: arrows). At P5

and P30, additional cells in the inner nuclear and ganglion cell layers showed robust nuclear localization of HDAC2. At P30 HDAC2 was also detected in Müller glial nuclei (Fig 4E: open arrows), although not as robustly as in amacrine cells and retinal astrocytes. Very weak, but consistent HDAC2 immunolabeling was detected in the outer nuclear layer at P30. Sections treated with preabsorbed antibody showed no HDAC2 label at any of the stages examined (Fig 4G-I).

2.3c HDAC3

Overall, HDAC3 expression patterns were similar to HDAC2, with primarily non-nuclear immunoreactivity at E16, increased nuclear staining in the inner nuclear and ganglion cell layers at P5 and P30. Weak HDAC3 labeling was observed in progenitor nuclei primarily at the sclerad edge of the retina at E16 (Fig 5A), whereas only a few scattered SOX2+ progenitor cells were co-labeled with HDAC3 at P5 (Fig 5C: open arrows).

At E16, only a subpopulation of RGCs nuclei, primarily those closest to the vitreous, showed weak HDAC3 immunoreactivity, whereas migrating RGCs were HDAC3 negative (Fig 5B; Supplementary Fig 3A, B). Nuclear HDAC3 immunoreactivity in RGCs increased at P5 (Fig 5D), and was still present at P30 (Fig 5F).

SOX2+ cholinergic amacrine cells (Fig 5C: closed arrows) and retinal astrocytes (Fig 5C: arrowheads) showed distinct nuclear localization of HDAC3, but only at P5 (Fig 5C). By P30, no HDAC3 label was present in Müller glial cells (Fig 5E; open arrows), HDAC3 label was present in the nuclei of cholinergic amacrine cells (Fig 5E; Supplementary Fig 3C, D: arrows in INL), and strong label was still apparent in the nuclei of retinal astrocytes (Fig 5E: arrowheads; Supplementary Fig 3C, D: arrows in GCL). Sections treated with preabsorbed antibody showed no HDAC3 label at any of the stages examined (Fig 5G-I).

2.3d HDAC8

HDAC8 immunoreactivity was primarily non-nuclear at E16 and P5. SOX2+ progenitor nuclei were devoid of HDAC8 signals at both E16 (Fig 6A) and P5 (Fig 6C: open arrows). Comparatively, RGC nuclei were consistently, albeit weakly positive for HDAC8 at E16 and P5 (Fig 6B, D; Supplementary Fig 4: arrows), but no HDAC8 immunostaining was present in RGC nuclei at P30 (Fig 6F). At P5, cholinergic amacrine cells (Fig 6C: arrows) and retinal astrocytes (Fig 6C: arrowheads) showed some nuclear co-labeling for SOX2 and HDAC8 (Supplementary Fig 5: arrows). Consistent with the low levels of HDAC8 levels seen in western blots, P30 retina

showed no detectable HDAC8 immunoreactivity (Fig 6E, F). Sections treated with preabsorbed antibody showed little HDAC8 label at any of the stages examined (Fig 6G-I).

3. Discussion

We observed dynamic changes in cellular patterns and sub-cellular localization of the different Class I HDACs during retinal development, despite only minor changes in total HDAC mRNA or protein levels (summarized in Tables 1 and 2). Of the HDACs analyzed, all showed at least some level of both nuclear and non-nuclear localization across developmental timepoints. HDAC1 was the only Class I HDAC that showed a primarily nuclear localization in early stage retinal progenitors, as well as in differentiated cells with in the inner nuclear and ganglion cell layers. In contrast, distinctly nuclear localization of HDAC2 and 3 was not detected in retinal progenitors, but was present in differentiated cells in the inner nuclear and ganglion cell layers at P5 and P30. HDAC8 was predominantly non-nuclear at E16 and P5, and was not detected by immunofluorescence at P30. Theoretically, a change in nuclear localization during key points of differentiation may indicate HDACs that are critical to the chromosomal organization that accompanies the loss of progenitor characteristics and/or the gain of differentiative characteristics.

While we focused primarily on nuclear localization of the HDACs, we noted in analyzing the data that each also showed cytoplasmic localization at one or more stages of development. Class I HDACs have widely been described as having predominantly nuclear localization (Barry and Townsend, 2010; Yano et al., 2018; Zahnow et al., 2016). However, careful review of the literature indicates that this most likely is not true and that Class I HDACs may have cell- or tissue-specific functions that require cytoplasmic localization (Guo et al., 2015; Hou et al., 2014; Seto and Yoshida, 2014; Takase et al., 2013; Waltregny et al., 2004; Yao and Yang, 2011). There was substantial label found in the inner plexiform layer for each of the HDACs at one or more stages with the exception of HDAC3. It is of interest to note that the inner plexiform layer is a synaptic area comprised primarily of axons and dendrites from bipolar, amacrine, and ganglion cells. HDAC1 and 2 are localized to post-synaptic densities in dendrites in many regions of the brain (Takase et al., 2013). HDACs 3 and 8 are also localized to post-synaptic densities, but in fewer regions of the brain than 1 and 2. HDAC2 has also been described in the hippocampus as having both nuclear and/or cytoplasmic localization, depending the stage examined (Hou et al., 2014).

A few of the timepoints we examined showed a low correlation between protein and mRNA levels (for instance HDAC8 levels at P30). While there can be good correlation between mRNA and protein level, particularly when protein half-life is short (Raj et al., 2006), evidence from other literature suggests the mRNA level is not predictive of protein level (Liu et al., 2016;

Taniguchi et al., 2010). There are many reasons why there may not be a relationship between mRNA and protein levels. For instance, post-transcriptional modifications (PTMs) such as micro RNAs can regulate degradation of mRNAs and reduce translation of proteins (Fabian et al., 2010). In addition, protein level can be affected by PTMs that alter protein half-life. While most investigators associate HDACs with reversal of a PTM to other proteins, HDACs are also targets of multiple types of PTMs, such as phosphorylation, methylation, ubiquitination, oxidation, sumoylation, nitrosylation, ADP-ribosylation, glycosylation, and carbonylation (Segre and Chiocca, 2011). Class I HDACs have much greater enzymatic activity than other HDACs and are also known to target many proteins in addition to histones, and so it has been proposed that both of these characteristics may be regulated by PTMs (Eom and Kook, 2014). Furthermore, Class I HDACs are known to be degraded in a PTM-dependent fashion (Adenuga et al., 2009; Choi et al., 2015; Park and Juhnn, 2017; Segre and Chiocca, 2011).

3.1 H3K9 acetylation in the retina

Histone acetylation is typically associated with open chromatin structure and active gene transcription. In embryonic stem (ES) cells, inhibition of H3K9 deacetylation maintains expression of pluripotency genes and blocks neuronal differentiation (Qiao et al., 2015). In contrast, H3K9 di- and tri-methylation is associated with silencing of pluripotency genes in neuroprogenitors derived from ES cells (Golebiewska et al., 2009). Therefore, it was unexpected that few retinal progenitors at E16 or P5 were stained for acetylated H3K9, whereas essentially all progenitors were stained for H3K9-me3. Early stage retinal progenitors had clearly detectible nuclear localization of HDAC1 throughout the neuroblastic layer at E16. Thus, it is likely that at least some level of active histone deacetylation occurs in neural retinal progenitors. Nevertheless, acetylation of other lysine residues on multiple histone proteins (e.g. H3K14, H4K8) is also associated with transcriptional activation and pluripotency (Agalioti et al., 2002). Because these other patterns of acetylation would not be detected using H3K9-ac specific antibodies used in our study, overall levels of histone acetylation in retinal progenitors is likely higher than our immunostaining would suggest. A recent study showed that 4 days of pharmacological inhibition of HDAC1 in P1 retinal explants increased H3K9 and H4K12 acetylation in both the inner and outer retina, although these studies did not analyze earlier timepoints (Ferreira et al., 2017). Thus, further studies will be required to determine the patterns and functional significance other histone acetylation and methylation motifs in early stage retinal progenitors.

3.2 Class I HDACs in retinal progenitors

In the retina, SOX2, a SOXB1-HMG box transcription factor, is required to keep retinal progenitors in the cell cycle and SOX2 expression is down-regulated as progenitors exit the cell cycle and differentiate (Taranova et al., 2006). Both Class I and Class III HDACs have been implicated in regulating SOX2 expression (Kondo and Raff, 2004; Lyssiotis et al., 2007; Staszkiewicz et al., 2013). Most HDACs repress SOX2 transcription in neural progenitors (Lyssiotis et al., 2007; Wang et al., 2015) and loss of HDAC2 activity, in particular, has been associated with an increase in SOX2 expression (Conway et al., 2012; Jawerka et al., 2010). We observed little to no expression of HDAC2, 3 or 8 in early stage retinal progenitors. Interestingly, HDAC1 had a distinctly nuclear localization in SOX2+ early stage retinal progenitors. In ES cells, HDAC1 and HDAC2 are required for positive regulation of several pluripotency genes and the promoters of *Oct4*, *Nanog* and *Sox2* are physically occupied by HDAC1 (Kidder and Palmer, 2012; Saunders et al., 2017). Thus, the expression of HDAC1 and absence of HDAC2 in early stage retinal progenitors could reflect a novel, HDAC2-independent role for HDAC1 in positive regulation of SOX2. Consistent with the idea that HDAC1 is compatible with SOX2 expression, HDAC1 was the only Class I HDAC that co-labeled SOX2+ Müller glial cells at P30.

HDACs also regulate cell cycle progression and the G1 to S phase transition is blocked in *Hdac1* -/- mice (Lagger et al., 2002), or by general inhibition of HDAC activity by suberoylanilide hydroxamic acid (SAHA) and sodium butyrate (Zhou et al., 2011). A more targeted study of HDAC1 and 2 in hematopoiesis indicates that they may function in both cell cycle progression and differentiation (Wilting et al., 2010). There is also evidence that HDAC1 knockout leads to increased levels of p21 and p27, as well as decreased levels of cyclins A and E in the embryo (Lagger et al., 2002). Interestingly, conditional knockout of both HDAC1 and HDAC2 in ES cells results in defects in chromosomal segregation during mitosis and a general cessation of proliferation, followed by cell death (Jamaladdin et al., 2014). This points to a critical role for HDAC1 and HDAC2 in mitosis, apart from their regulation of the G1 to S transition. Consistent with this, HDAC1 inhibition in post-natal retinal explants decreases BrdU incorporation (Ferriera 2017). The robust nuclear expression of HDAC1 in early-stage retinal progenitors could reflect an additional role in maintaining proliferative capacity and expression of genes associated with multipotency.

When results of HDAC inhibition are considered in the context of the complementary expression patterns of HDAC1 and H3K9ac, these data suggest that histone deacetylation by HDAC1 plays an active role in retinal progenitors. Interestingly, pharmacological inhibition of HDAC1 in P1 retinal explants also increases expression of some retinal progenitor and cell cycle associated genes (e.g. *Hes1, Vsx2, Ccnd1*), and decreases expression of rod photoreceptor-specific genes (e.g. rhodopsin, *Nrl*, *Pde6b*) (Ferriera 2017). Thus, it is tempting to speculate that changes in histone acetylation and HDAC1 expression in early vs. late stage progenitors contribute to developmental changes in their neurogenic competence.

3.3 Class I HDACs in differentiating neurons

Histone deacetylation plays a key role in regulating expression of pluripotency genes and the switch towards neural differentiation, but the mechanisms by which HDACs regulate proliferation and/or differentiation have been studied in tissues other than the retina. In differentiating RGCs at E16, nuclear HDAC1 immunoreactivity progressively increased in post-mitotic retinal ganglion cells as they migrated towards the ganglion cell layer. In contrast, overall levels of HDAC2 and 3 in differentiating retinal ganglion cells were much lower at E16. Nevertheless, HDAC1, HDAC 2 and HDAC3 all showed robust nuclear staining in neurons located in both the inner nuclear and ganglion cell layers at P5, again pointing to a role for histone deacetylation in differentiation of retinal neurons. HDAC1, 2, and 3 expression was also fairly robust in the ganglion cell layer at P30, suggesting that continued expression of these HDACs may be required for maintenance of neuronal differentiation.

3.4 Class I HDACs in retinal glia

There appear to be cell-type specific roles for HDACs in neurogenesis vs. gliogenesis. For example, HDAC inhibition blocks neurogenesis and promotes gliogenesis by neural progenitors derived from embryonic ganglionic eminence, but has the opposite effect on neural progenitors from the embryonic cortex (Shaked et al., 2008). We observed that all 4 Class I HDACs were expressed in the nuclei of retinal astrocytes at P5 and HDAC1, 2, and 3 were present at P30. However, only HDAC1 was present in Müller glia. These two cell types are derived from different lineages, with astrocytes migrating into the retina from progenitors located in the optic stalk (Chan-Ling and Stone, 1991; Otteson et al., 1998; Zhang and Stone, 1997). We previously

showed that the SOX2+ astrocyte precursors in the optic nerve also express HDACs 1, 2 and 3 at E16 (Tiwari et al., 2014). In contrast, Müller glia are the progeny of retinal progenitors and share lineage relationship with retinal neurons. Interestingly, Müller glia express many of the same genes as retinal progenitors and show limited stem-cell characteristics in the mammalian retina following injury and growth factor stimulation (Beach et al., 2017; Bernardos et al., 2007; Goldman, 2014; Otteson et al., 2001; Otteson and Phillips, 2010; Vihtelic and Hyde, 2000; Yao et al., 2018). A recent study showed that overexpression of activated β-catenin and CRX/NRL induced Müller glia to reenter the cell cycle and generate new rod photoreceptors in the absence of injury, further supporting the stem cell-like characteristics of Müller glia (Yao et al., 2018). The expression of HDAC1 in both Müller glia and early-stage retinal progenitors may be reflect the shared characteristics of these cells.

In conclusion, the expression patterns of Class I HDACs were consistent with the idea that these proteins may play significant roles in the differentiation of neurons and glia within the retina. The robust and continued expression of HDACs 1, 2, and 3 in differentiated neurons is likely to reflect important roles in the maturation, maintenance of differentiation, and cellular functions of multiple cell-types within the retina. Future studies will be directed at inhibition and/or knockout of specific HDACs at multiple stages during retinal development to determine their role in the specification, differentiation and maintenance of other retinal cell types. The potential role of other classes of HDACs also need to be considered in retinal differentiation and/or maintenance; however, inhibition of Class III HDACs had minimal effect on H3K9, H3K27 or H4K12 acetylation in retinal explants (Ferreira et al., 2017). Deacetylation by HDACs can regulate function of multiple proteins inside and outside the nucleus in other tissues (Li et al., 2014), and it will undoubtedly be informative to identify additional HDAC substrates and their functions in the retina. Finally, histone methylation, which is closely associated with histone deacetylation by HDACs, also needs further clarification in its role in retinal differentiation.

4. Materials and Methods

4.1 Animals used in the study and tissue harvest

All experiments in this study conformed to the guidelines from the National Institutes of Health Guide for the Care and Use of Laboratory Animals, Eighth Edition (NIH Publications No. 8023) and were approved by the IUPUI School of Science IACUC. C57BL/6J mice from Jackson Labs (Bar Harbor, ME) were maintained on a 12 hour light/dark cycle and mated within the facility. For embryonic tissue, the date of vaginal plug was designated as 0.5 days post coitum. Whole heads from embryonic day 16 (E16) and eyes from postnatal stages (P5) were fixed between 1:00 and 3:00pm using 4% paraformaldehyde in 0.1 M phosphate buffer, pH 7.4 at 4°C overnight. P30 eyes were fixed in 4% paraformaldehyde in 0.1M cacodylate buffer (pH 7.4) for 1 hour at 4°C. Tissue was then rinsed in phosphate buffered saline (PBS: potassium chloride 200 mg/L, potassium phosphate 200 mg/L, sodium chloride 8000 mg/L, and sodium phosphate 1150 mg/L), pH 7.5 and infiltrated with a gradient of sucrose in 0.1 M phosphate buffer, from 5% to 20% over 4 days. Eyes were frozen a 3:1 ratio of 20% sucrose in 0.1 M phosphate buffer to Optimal Cutting Temperature (OCT; Sakura Finetek USA Inc) solution and retinal sections cut twelve microns (Leica CM3050 S cryostat) were mounted on charged glass slides (Superfrost plus™) and stored at -70°C.

4.2 Immunohistochemistry

Concentrations of primary and secondary antibodies used in this study are listed in the Key Resources Table. Immunohistochemistry was performed as described in Tiwari *et al*. (Tiwari et al., 2014). Briefly, slides with cryosections were post-fixed using 4% paraformaldehyde (30 min, room temperature). Slides were rinsed in PBS and permeabilized with methanol (10 min), followed by antigen retrieval (1% SDS in 0.01M PBS) for 5 min. To reduce autofluorescence, slides were incubated in 1% sodium borohydride (Acros, New Jersey) in PBS (2-5 min). Non-specific binding was blocked by incubation in PBS containing 0.25% TritonX-100 (Biorad, Hercules, CA) and 10% normal donkey serum (30 min). Primary antibodies were diluted in PBS with 2% donkey serum, 0.025% TritonX-100 and incubated overnight at 4°C. Secondary antibodies were Alexa-fluor conjugated (Donkey anti-rabbit 549 and Donkey anti-mouse 546; Invitrogen) or DyLight conjugated (Donkey anti-goat 488; Jackson ImmunoResearch) were applied for 1 hr. Counterstaining for nuclei was performed using 2µg/ml of Hoechst Stain (Cat# H1399, Invitrogen). Slides were coverslipped by using Aquamount (Cat#18606-20,

Polysciences Inc; Warrington, PA). Slides were imaged using an Olympus Confocal FV 1000 microscope. Each antibody label was analyzed on sections through at least 3 separate eyes at each stage.

To test the specificity of the primary antibodies used, some sections were stained using antibodies pre-absorbed with specific peptides (sourced from antibody supplier or made by Thermofisher) to each HDAC antibody. Each antibody was preabsorbed with the relevant peptide for one hour before applying to the tissue of interest. To test for non-specific background staining of the secondary antibody, IgG controls were done wherein tissue sections were incubated with the IgG of the host (Thermofisher) in which the primary antibody was made (Supplementary Figure 1), in place of the primary antibody incubation. Subsequent steps of the immunostaining procedures peptide and IgG controls followed the standard protocol both described above.

4.3 Western blot analysis

Immunoblotting was performed as described in Tiwari *et al* using antibodies at the concentrations described in Key Resources Table (Tiwari et al., 2014). Briefly, retinas from three stages of development (E16, P5 and P30) were lysed in lysis buffer (5M NaCl, 1M Tris pH 8.0, 0.5 M EDTA, 5% TritonX-100), containing protease inhibitor cocktail (cOmplete™; Roche) and 1 mM phenylmethanesulfonylfluoride (PMSF), and quantified using bicinchoninic acid assays (Pierce BCA Protein Assay Kit; Thermoscientific) and spectrophotometer (NanoDrop 2000c; ThermoFisher Scientific) following manufacturer's instructions. For western blots, 50 µg total protein was mixed with the laemmli sample buffer loading dye at 3:1 ratio, incubated at 65°C for 15 minutes and 50 µg per lane loaded and separated on SDS-PAGE (4-20% gradient gel) at 150 V for approximately one hour prior to transfer to polyvinylidene difluoride (PVDF) membrane in transfer buffer containing 25mM Tris, 192mM glycine, pH8.3 and 20% methanol. Non-specific binding to membranes was blocked for one hour prior to application of antibodies. For most antibodies, protein-free blocking buffer (Pierce Protein–Free T20 (TBS) Blocking Buffer, Cat# 37571) was used. For antibodies specific to HDAC2 Tris-buffered saline-Tween (TBST: 20 mM Tris base, 137 mM sodium chloride, 1 M HCl, 0.1% Tween-20, at pH 7.6) containing 5% non-fat dry milk was used for blocking. Membranes were subsequently probed using same antibodies as used as used for immunohistochemistry, specific to each of the HDACs, diluted in corresponding blocking buffer and incubated overnight at 4°C on a shaker. Blots were washed with TBST, followed by incubation with peroxidase-conjugated secondary

antibodies (ThermoFisher Scientific) diluted 1:5000 in TBST for 1 hour at room temperature. Bands were detected via chemiluminescence (Super Signal West Femto Chemiluminescent Substrate; Thermoscientific) and photosensitive film. Antibodies and concentrations used for Western blots are listed in Table 3. β-tubulin was used as a loading control. Quantification used Image J 1.34 software for densitometry. Statistical analysis used one-way ANOVA, with post-hoc pairwiseT-tests corrected for multiple comparisons using the Bonferroni method (GraphPad Prism software, v5.0; GraphPad Software, Inc., San Diego, CA), with $p \leq 0.05$ considered statistically significant.

4.4 RT-qPCR

Retinal tissue was isolated from eyes of mice from three stages of development (E16, P5, and P30), and preserved with an RNA stabilization reagent (Cat#76104, Qiagen). Tissue samples were stored -70°C for no more than 2 months prior to RNA isolation. Total RNA was isolated using affinity columns (RNeasyPlus mini kit # 74134; Qiagen) as per manufacturer's instructions, with samples eluted in 40µl of RNAse-free water and stored at -80°C until reverse transcription. Total RNA was quantified by spectrophotometry (Nanodrop 2000c; ThermoFisher Scientific). cDNA was reverse transcribed from 1µg total RNA (iScript cDNA synthesis kit # 170-8891; Bio-Rad) using a proprietary blend of oligo(dT) primers and random hexamers, as per manufacturers protocol. The sequences and efficiencies of all primer pairs used have been previously described (Tiwari et al., 2014). Quantitative PCR reactions were performed in triplicate 20µl reactions using SYBR green chemistry (Cat# 04707516001; Roche) in the Light Cycle 480 II system (Roche). Cycling conditions were: initial denaturation at 95˚C, 10 minutes (min); followed by 40 cycles of 95˚C for 10 seconds (sec), 60˚C for 30 sec, and 72˚C for 30 sec; and a final extension of 72˚C for 5 min. Melting curve analysis was performed with each PCR reaction to verify single products were generated. Three reference genes were used for normalization: β-2 microglobulin (*β2m*), signal recognition particle 14kDa (*Srp14*) and succinate dehydrogenase complex, subunit A (*Sdha*) (Tiwari et al., 2014). Relative expression software tool-multiple condition solver (REST-MCS (Pfaffl et al., 2002)) was used for data analysis to determine relative expression and statistical significance of changes (Tiwari et al., 2014). For each timepoint, at least three biological replicates were analyzed by RT-qPCR.

Figure Legends

Figure 1: Localization of acetylated and tri-methylated histone H3 (K9) in murine retina. Confocal images of acetylated histone H3 (H3K9ac) and tri-methylated H3 (H3K9me3) and Hoechst (blue) triple-label of murine retina at E16 (A-C), P5 (D-F) and P30 (G-I). (A) H3K9ac label was found in progenitors at the sclerad edge of the E16 neuroepithelium (arrows) and presumptive astrocytes at the vitreal edge of the optic cup (arrowheads) at E16. Non-specific label was detected in the sclerad basal laminae at E16 (See Supplementary Figure 5 for controls) (D & G) Progenitors at the sclerad edge of the developing retina remain at P5, but no label was apparent at P30. (B, C, E, F) H3Kme3 immunolabel was present throughout the E16 and P5 retina, and co-labeled H3K9ac+ cells. (H & I) H3K9me3 was retained throughout the retina at P30, but was weaker than E16 and P5 label. No co-labeled cells were present at P30. Scale bar in (A) = 50 µm for A-C. Scale bar in (D) = 50µm scale bar for D-I. Abbreviations: RPE, retinal pigmented epithelium; NBL, neuroblast layer; INL, inner nuclear layer; ONL, outer nuclear layer; GCL, ganglion cell layer.

Figure 2: mRNA and protein levels of Class I HDACs during retinal development.
(A) Levels of *Hdacs1, 2, 3, and 8* were analyzed using RT-qPCR at E16, P5, and P30 relative to E16. All Class I *Hdacs* were expressed at all stages of developing retina in this study. Bars show mean log (2) fold change ± SEM of three biological samples per time point. ***, $p = 0.001$ vs. E16. (B) Western blot analysis for Class I HDACs was performed and levels analyzed by densitometry using β-tubulin as a loading control. Bars show mean ± SEM of three samples per time point. An ANOVA analysis indicated that changes in protein levels did not reach the level of statistical significance.

Figure 3: Localization of HDAC1 in developing murine retina.
Sections from E16 (A, B), P5 (C, D) and P30 (E, F) of developing murine retina were double-labeled for HDAC1 and SOX2 (A, C, E), POU4F3 (B, D), or POU4F1 (F) to determine nuclear colocalization. (C) Open arrows indicate SOX2+ progenitors, closed arrows indicate cholinergic amacrine cells, arrowheads indicate retinal astrocytes, and asterisks indicate suspected horizontal cells. (E) Open arrows indicate Müller glial cells, closed arrows indicate cholinergic amacrine cells, arrowheads represent retinal astrocytes, and asterisks indicate suspected horizontal cells. Sections through E16 (G), P5 (H), and P30 (I) retina treated with antibody preabsorbed with HDAC1 peptide were devoid of signal. Scale bar in (A) = 50 µm for A-F. Scale

bar in (G) = 50μm scale bar for G-I. Abbreviations: RPE, retinal pigmented epithelium; NBL, neuroblast layer; INL, inner nuclear layer; ONL, outer nuclear layer; GCL, ganglion cell layer.

Figure 4: Localization of HDAC2 in developing murine retina.

Sections from E16 (A, B), P5 (C, D) and P30 (E, F) of developing murine retina were double-labeled for HDAC2 and SOX2 (A, C, E), HDAC2 and POU4F3 (B, D), or HDAC2 and POU4F1 (F). Open arrows indicate retinal progenitors in A, B, and C. Arrowheads (A) indicate retinal astrocytes. (B) Arrowheads designate migrating RGCs, while arrows indicate RGCs in the ganglion cell layer (GCL). (C) Closed arrows indicate cholinergic amacrine cells, and arrowheads indicate retinal astrocytes. (E) Open arrows indicate Müller glial cells, closed arrows show cholinergic amacrine cells, and arrowheads designate retinal astrocytes. Peptide controls in which the antibody was preabsorbed with the corresponding peptide was performed (G, H and I). Scale bar in (A) = 50 μm for A-F. Scale bar in (G) = 50μm scale bar for G-I. Abbreviations: RPE, retinal pigmented epithelium; NBL, neuroblast layer; INL, inner nuclear layer; ONL, outer nuclear layer; GCL, ganglion cell layer; OPL, outer plexiform layer; IPL, inner plexiform layer.

Figure 5: Localization of HDAC3 in developing murine retina.

Sections from E16 (A, B), P5 (C, D) and P30 (E, F) of developing murine retina were double-labeled for HDAC3 and SOX2 (A, C, E), or HDAC3 and POU4F3 (B, D), or HDAC3 and POU4F1 (F). (C) Open arrows indicate SOX2+ progenitors, closed arrows indicate cholinergic amacrine cells, and arrowheads indicate retinal astrocytes. (E) Open arrows indicate Müller glial cells, closed arrows indicate cholinergic amacrine cells, and arrowheads represent retinal astrocytes. Peptide controls in which the antibody was preabsorbed with the corresponding peptide was performed (G, H and I). Scale bar in (A) = 50 μm for A-F. Scale bar in (G) = 50μm scale bar for G-I. Abbreviations: RPE, retinal pigmented epithelium; NBL, neuroblast layer; INL, inner nuclear layer; ONL, outer nuclear layer; GCL, ganglion cell layer; OPL, outer plexiform layer; IPL, inner plexiform layer.

Figure 6: Localization of HDAC8 in developing murine retina.

Sections for E16 (A, B), P5 (C, D) and P30 (E, F) of developing murine retina were double-labeled for HDAC8 and SOX2 (A, C, E), or HDAC 8 and POU4F3 (B, D), or HDAC8 and POU4F1 (F) to determine nuclear co-localization. (C) Open arrows indicate SOX2+ progenitors, closed arrows indicate cholinergic amacrine cells, and arrowheads indicate retinal astrocytes.

Peptide controls in which the antibody was preabsorbed with the corresponding peptide was performed (G, H and I). Scale bar in (A) = 50 µm for A-F. Scale bar in (G) = 50µm scale bar for G-I. Abbreviations: RPE, retinal pigmented epithelium; NBL, neuroblast layer; INL, inner nuclear layer; ONL, outer nuclear layer; GCL, ganglion cell layer; OPL, outer plexiform layer; IPL, inner plexiform layer.

Supplementary Figure 1: IgG negative controls.
To determine non-specific binding of secondary antibodies, sections from E16 (A, D), P5 (B, E), and P30 (C, F) retina were reacted with isotypic IgG in place of primary antibody followed by fluorescently conjugated secondary antibodies. Scale bar in (A) = 50µm scale bar for A-D.

Supplementary Figure 2: Channel separated enlarged views of HDAC1.
Sections through E16 murine retina were double-labeled for HDAC1 (A) and SOX2 (B) or HDAC1 (C) and POU4F3 (D). Arrows indicate cells that were co-labeled, while arrowheads indicate cells that were labeled for HDAC1 (A, C), but not for the accompanying cell type-specific label (B, D). Scale bar in (A) = 50µm scale bar for A-D.

Supplementary Figure 3: Channel separated enlarged views of HDAC3.
Sections through E16 (A, B) or P30 (C, D) murine retina were double-labeled for HDAC3 (A) and POU4F3 (B) or HDAC3 (C) and SOX2 (D). Arrows indicate cells that were co-labeled, while arrowheads indicate cells that were labeled for HDAC3 (C), but not for SOX2 (D). Scale bar in (A) = 50µm scale bar for A-D.

Supplementary Figure 4: Channel separated enlarged views of HDAC8 at E16 and P5.
Sections through E16 (A, B) or P5 (C, D) murine retina were double-labeled for HDAC8 (A, C) and POU4F3 (B, D). Arrows indicate cells that were co-labeled. Scale bar in (A) = 50µm scale bar for A-D.

Supplementary Figure 5: Channel separated enlarged views of HDAC8 at P30.
Sections through P5 murine retina were double-labeled for HDAC8 (A) and SOX2 (B). Arrows indicate cells that were co-labeled. Scale bar in (A) = 50µm scale bar for A-B.

List of Abbreviations

ANOVA	analysis of variance
ARVO	Association for Research in Vision and Ophthalmology
BCA	bicinchoninic acid
bHLH	basic helix-loop-helix
CNS	central nervous system
ES	cells embryonic stem cells
E16	embryonic day 16
GABA	gamma-Aminobutyric acid
GCL	ganglion cell layer
H3K9ac	acetylated histone H3 at lysine 9
H3K9me3	tri-methylated histone H3 at lysine 9
H3K14	histone H3 lysine 14
H4K8	histone H4 lysine 8
H4K12	histone H4 lysine 12
HATs	histone acetyl transferases
HDACs	histone deacetylases
INL	inner nuclear layer
IPL	inner plexiform layer
IUPUI	Indiana University Purdue University at Indianapolis
min	minutes
mRNA	messenger ribonucleic acid
NAD	nicotinamide adenine dinucleotide
NBL	neuroblast layer
NCoR	nuclear receptor corepressor
NuRD	nucleosome remodeling deacetylase
OCT	Optimal Cutting Temperature
ONL	outer nuclear layer
OPL	outer plexiform layer

P5	postnatal day 5
P30	postnatal day 30
PBS	phosphate buffered saline
PMSF	phenylmethanesulfonylfluoride
PVDF	polyvinylidene difluoride
REST	RE1-silencing transcription factor complex
REST-MCS	Relative expression software tool-multiple condition solver
RGCs	retinal ganglion cells
RPCs	retinal progenitor cells
RPE	retinal pigmented epithelium
RT-qPCR	reverse transcriptase-quantitative polymerase chain reaction
SAHA	suberoylanilide hydroxamic acid
SDS-PAGE	sodium dodecyl sulfate polyacrylamide gel electrophoresis
sec	seconds
SHIP1	spermatogenic HDAC-interacting protein 1
SIRT	NAD+ dependent sirtuins
SMRT	silencing mediator for retinoid and thyroid receptors
TBST	Tris-buffered saline-Tween
W	West

Declarations

Ethics approval: All experiments in this study conformed to the guidelines from the National Institutes of Health Guide for the Care and Use of Laboratory Animals, Eighth Edition (NIH Publications No. 8023) and were housed in an AAALAC accredited housing facility in the IUPUI School of Science. The ethical treatment of animals used for this study was approved by the IUPUI Science Animal Resource Center (protocol SC194R).

Competing interests

The authors declare no competing interests.

Authors' contribution

Experimental conception and design: TLBA, DCO, AS

Performance of experiments: AS, ST, SD, TLBA

Analysis of results: TLBA, DCO, AS, ST, SD

Manuscript preparation: TLBA, DCO, AS, ST, SD

All authors read and approved the final manuscript.

Acknowledgements

The authors would like to gratefully acknowledge funding sources that supported this work: National Eye Institute R01EY019525-02 and R15EY020816-01 to TLBA (for data generation, collection, and analysis; for writing of manuscript), and R01EY021792 to DCO (for data analysis and writing of manuscript).

References

Adenuga, D., Yao, H., March, T.H., Seagrave, J., Rahman, I., 2009. Histone deacetylase 2 is phosphorylated, ubiquitinated, and degraded by cigarette smoke. Am. J. Respir. Cell Mol. Biol. 40, 464-473, 10.1165/rcmb.2008-0255OC.
Agalioti, T., Chen, G., Thanos, D., 2002. Deciphering the transcriptional histone acetylation code for a human gene. Cell 111, 381-392, http://www.ncbi.nlm.nih.gov/pubmed/12419248
Bannister, A.J., Kouzarides, T., 2011. Regulation of chromatin by histone modifications. Cell Res 21, 381-395, 10.1038/cr.2011.22.
Barry, S.P., Townsend, P.A., 2010. What causes a broken heart--molecular insights into heart failure. Int. Rev. Cell Mol. Biol. 284, 113-179, 10.1016/S1937-6448(10)84003-1.
Beach, K.M., Wang, J., Otteson, D.C., 2017. Regulation of Stem Cell Properties of Muller Glia by JAK/STAT and MAPK Signaling in the Mammalian Retina. Stem Cells Int 2017, 1610691, 10.1155/2017/1610691.
Bernardos, R.L., Barthel, L.K., Meyers, J.R., Raymond, P.A., 2007. Late-stage neuronal progenitors in the retina are radial Muller glia that function as retinal stem cells. J. Neurosci. 27, 7028-7040, 10.1523/JNEUROSCI.1624-07.2007.
Brown, N.L., Patel, S., Brzezinski, J., Glaser, T., 2001. Math5 is required for retinal ganglion cell and optic nerve formation. Development 128, 2497-2508, http://www.ncbi.nlm.nih.gov/pubmed/11493566
Brzezinski, J.A.t., Brown, N.L., Tanikawa, A., Bush, R.A., Sieving, P.A., Vitaterna, M.H., Takahashi, J.S., Glaser, T., 2005. Loss of circadian photoentrainment and abnormal retinal electrophysiology in Math5 mutant mice. Invest. Ophthalmol. Vis. Sci. 46, 2540-2551, 10.1167/iovs.04-1123.
Brzezinski, J.A.t., Prasov, L., Glaser, T., 2012. Math5 defines the ganglion cell competence state in a subpopulation of retinal progenitor cells exiting the cell cycle. Developmental biology 365, 395-413, 10.1016/j.ydbio.2012.03.006.
Chan-Ling, T., Stone, J., 1991. Factors determining the migration of astrocytes into the developing retina: migration does not depend on intact axons or patent vessels. J. Comp. Neurol. 303, 375-386, 10.1002/cne.903030304.
Chen, B., Cepko, C.L., 2007. Requirement of histone deacetylase activity for the expression of critical photoreceptor genes. BMC developmental biology 7, 78, 10.1186/1471-213X-7-78.
Chen, B., Cepko, C.L., 2009. HDAC4 regulates neuronal survival in normal and diseased retinas. Science 323, 256-259, 10.1126/science.1166226.
Chen, H.P., Zhao, Y.T., Zhao, T.C., 2015. Histone deacetylases and mechanisms of regulation of gene expression. Crit Rev Oncog 20, 35-47, http://www.ncbi.nlm.nih.gov/pubmed/25746103
Choi, H.K., Choi, Y., Park, E.S., Park, S.Y., Lee, S.H., Seo, J., Jeong, M.H., Jeong, J.W., Jeong, J.H., Lee, P.C., Choi, K.C., Yoon, H.G., 2015. Programmed cell death 5 mediates HDAC3 decay to promote genotoxic stress response. Nat Commun 6, 7390, 10.1038/ncomms8390.
Conway, G.D., O'Bara, M.A., Vedia, B.H., Pol, S.U., Sim, F.J., 2012. Histone deacetylase activity is required for human oligodendrocyte progenitor differentiation. Glia 60, 1944-1953, 10.1002/glia.22410.
Cvekl, A., Mitton, K.P., 2010. Epigenetic regulatory mechanisms in vertebrate eye development and disease. Heredity (Edinb) 105, 135-151, 10.1038/hdy.2010.16.
Delcuve, G.P., Khan, D.H., Davie, J.R., 2013. Targeting class I histone deacetylases in cancer therapy. Expert Opin Ther Targets 17, 29-41, 10.1517/14728222.2013.729042.
Du, J., Johnson, L.M., Jacobsen, S.E., Patel, D.J., 2015. DNA methylation pathways and their crosstalk with histone methylation. Nat Rev Mol Cell Biol 16, 519-532, 10.1038/nrm4043.
Eberhart, A., Feodorova, Y., Song, C., Wanner, G., Kiseleva, E., Furukawa, T., Kimura, H., Schotta, G., Leonhardt, H., Joffe, B., Solovei, I., 2013. Epigenetics of eu- and heterochromatin in inverted and conventional nuclei from mouse retina. Chromosome Res 21, 535-554, 10.1007/s10577-013-9375-7.

Elliott, J., Jolicoeur, C., Ramamurthy, V., Cayouette, M., 2008. Ikaros confers early temporal competence to mouse retinal progenitor cells. Neuron 60, 26-39, 10.1016/j.neuron.2008.08.008.
Eom, G.H., Kook, H., 2014. Posttranslational modifications of histone deacetylases: implications for cardiovascular diseases. Pharmacol. Ther. 143, 168-180, 10.1016/j.pharmthera.2014.02.012.
Fabian, M.R., Sonenberg, N., Filipowicz, W., 2010. Regulation of mRNA translation and stability by microRNAs. Annu. Rev. Biochem. 79, 351-379, 10.1146/annurev-biochem-060308-103103.
Ferreira, R.C., Popova, E.Y., James, J., Briones, M.R., Zhang, S.S., Barnstable, C.J., 2017. Histone Deacetylase 1 Is Essential for Rod Photoreceptor Differentiation by Regulating Acetylation at Histone H3 Lysine 9 and Histone H4 Lysine 12 in the Mouse Retina. The Journal of biological chemistry 292, 2422-2440, 10.1074/jbc.M116.756643.
Gan, L., Xiang, M., Zhou, L., Wagner, D.S., Klein, W.H., Nathans, J., 1996. POU domain factor Brn-3b is required for the development of a large set of retinal ganglion cells. Proc. Natl. Acad. Sci. U. S. A. 93, 3920-3925, http://www.ncbi.nlm.nih.gov/pubmed/8632990
Gao, L., Cueto, M.A., Asselbergs, F., Atadja, P., 2002. Cloning and functional characterization of HDAC11, a novel member of the human histone deacetylase family. The Journal of biological chemistry 277, 25748-25755, 10.1074/jbc.M111871200.
Georgi, S.A., Reh, T.A., 2010. Dicer is required for the transition from early to late progenitor state in the developing mouse retina. J. Neurosci. 30, 4048-4061, 10.1523/JNEUROSCI.4982-09.2010.
Goldman, D., 2014. Muller glial cell reprogramming and retina regeneration. Nature reviews. Neuroscience 15, 431-442, 10.1038/nrn3723.
Golebiewska, A., Atkinson, S.P., Lako, M., Armstrong, L., 2009. Epigenetic landscaping during hESC differentiation to neural cells. Stem Cells 27, 1298-1308, 10.1002/stem.59.
Graw, J., 2010. Eye development. Current topics in developmental biology 90, 343-386, 10.1016/S0070-2153(10)90010-0.
Gregoretti, I.V., Lee, Y.M., Goodson, H.V., 2004. Molecular evolution of the histone deacetylase family: functional implications of phylogenetic analysis. J Mol Biol 338, 17-31, 10.1016/j.jmb.2004.02.006.
Guo, X., Ruan, H., Li, X., Qin, L., Tao, Y., Qi, X., Gao, J., Gan, L., Duan, S., Shen, W., 2015. Subcellular Localization of Class I Histone Deacetylases in the Developing Xenopus tectum. Front. Cell. Neurosci. 9, 510, 10.3389/fncel.2015.00510.
Haberland, M., Montgomery, R.L., Olson, E.N., 2009. The many roles of histone deacetylases in development and physiology: implications for disease and therapy. Nat Rev Genet 10, 32-42, 10.1038/nrg2485.
Harrison, M.R., Georgiou, A.S., Spaink, H.P., Cunliffe, V.T., 2011. The epigenetic regulator Histone Deacetylase 1 promotes transcription of a core neurogenic programme in zebrafish embryos. BMC Genomics 12, 24, 10.1186/1471-2164-12-24.
Hou, N., Gong, M., Bi, Y., Zhang, Y., Tan, B., Liu, Y., Wei, X., Chen, J., Li, T., 2014. Spatiotemporal expression of HDAC2 during the postnatal development of the rat hippocampus. Int. J. Med. Sci. 11, 788-795, 10.7150/ijms.8417.
Hufnagel, R.B., Le, T.T., Riesenberg, A.L., Brown, N.L., 2010. Neurog2 controls the leading edge of neurogenesis in the mammalian retina. Developmental biology 340, 490-503, 10.1016/j.ydbio.2010.02.002.
Iida, A., Shinoe, T., Baba, Y., Mano, H., Watanabe, S., 2011. Dicer plays essential roles for retinal development by regulation of survival and differentiation. Invest. Ophthalmol. Vis. Sci. 52, 3008-3017, 10.1167/iovs.10-6428.
Jamaladdin, S., Kelly, R.D., O'Regan, L., Dovey, O.M., Hodson, G.E., Millard, C.J., Portolano, N., Fry, A.M., Schwabe, J.W., Cowley, S.M., 2014. Histone deacetylase (HDAC) 1 and 2 are essential for accurate cell division and the pluripotency of embryonic stem cells. Proceedings of the National Academy of Sciences of the United States of America 111, 9840-9845, 10.1073/pnas.1321330111.

Jawerka, M., Colak, D., Dimou, L., Spiller, C., Lagger, S., Montgomery, R.L., Olson, E.N., Wurst, W., Gottlicher, M., Gotz, M., 2010. The specific role of histone deacetylase 2 in adult neurogenesis. Neuron Glia Biol 6, 93-107, 10.1017/S1740925X10000049.
Jaworska, J., Ziemka-Nalecz, M., Zalewska, T., 2015. Histone deacetylases 1 and 2 are required for brain development. Int J Dev Biol 59, 171-177, 10.1387/ijdb.150071tz.
Jiang, Y., Ding, Q., Xie, X., Libby, R.T., Lefebvre, V., Gan, L., 2013. Transcription factors SOX4 and SOX11 function redundantly to regulate the development of mouse retinal ganglion cells. J. Biol. Chem. 288, 18429-18438, 10.1074/jbc.M113.478503.
Karmodiya, K., Krebs, A.R., Oulad-Abdelghani, M., Kimura, H., Tora, L., 2012. H3K9 and H3K14 acetylation co-occur at many gene regulatory elements, while H3K14ac marks a subset of inactive inducible promoters in mouse embryonic stem cells. BMC Genomics 13, 424, 10.1186/1471-2164-13-424.
Kidder, B.L., Palmer, S., 2012. HDAC1 regulates pluripotency and lineage specific transcriptional networks in embryonic and trophoblast stem cells. Nucleic Acids Res 40, 2925-2939, 10.1093/nar/gkr1151.
Kiyama, T., Mao, C.A., Cho, J.H., Fu, X., Pan, P., Mu, X., Klein, W.H., 2011. Overlapping spatiotemporal patterns of regulatory gene expression are required for neuronal progenitors to specify retinal ganglion cell fate. Vision Res. 51, 251-259, 10.1016/j.visres.2010.10.016.
Kondo, T., Raff, M., 2004. Chromatin remodeling and histone modification in the conversion of oligodendrocyte precursors to neural stem cells. Genes Dev 18, 2963-2972, 10.1101/gad.309404.
Kong, Y., Jung, M., Wang, K., Grindrod, S., Velena, A., Lee, S.A., Dakshanamurthy, S., Yang, Y., Miessau, M., Zheng, C., Dritschilo, A., Brown, M.L., 2011. Histone deacetylase cytoplasmic trapping by a novel fluorescent HDAC inhibitor. Molecular cancer therapeutics 10, 1591-1599, 10.1158/1535-7163.MCT-10-0779.
La Torre, A., Georgi, S., Reh, T.A., 2013. Conserved microRNA pathway regulates developmental timing of retinal neurogenesis. Proc. Natl. Acad. Sci. U. S. A. 110, E2362-2370, 10.1073/pnas.1301837110.
Lagger, G., O'Carroll, D., Rembold, M., Khier, H., Tischler, J., Weitzer, G., Schuettengruber, B., Hauser, C., Brunmeir, R., Jenuwein, T., Seiser, C., 2002. Essential function of histone deacetylase 1 in proliferation control and CDK inhibitor repression. EMBO J 21, 2672-2681, 10.1093/emboj/21.11.2672.
Li, T., Song, B., Wu, Z., Lu, M., Zhu, W.G., 2014. Systematic identification of Class I HDAC substrates. Brief Bioinform 15, 963-972, 10.1093/bib/bbt060.
Liu, Y., Beyer, A., Aebersold, R., 2016. On the Dependency of Cellular Protein Levels on mRNA Abundance. Cell 165, 535-550, 10.1016/j.cell.2016.03.014.
Lyssiotis, C.A., Walker, J., Wu, C., Kondo, T., Schultz, P.G., Wu, X., 2007. Inhibition of histone deacetylase activity induces developmental plasticity in oligodendrocyte precursor cells. Proceedings of the National Academy of Sciences of the United States of America 104, 14982-14987, 10.1073/pnas.0707044104.
Mao, C.A., Kiyama, T., Pan, P., Furuta, Y., Hadjantonakis, A.K., Klein, W.H., 2008a. Eomesodermin, a target gene of Pou4f2, is required for retinal ganglion cell and optic nerve development in the mouse. Development 135, 271-280, 10.1242/dev.009688.
Mao, C.A., Wang, S.W., Pan, P., Klein, W.H., 2008b. Rewiring the retinal ganglion cell gene regulatory network: Neurod1 promotes retinal ganglion cell fate in the absence of Math5. Development 135, 3379-3388, 10.1242/dev.024612.
Marquardt, T., Ashery-Padan, R., Andrejewski, N., Scardigli, R., Guillemot, F., Gruss, P., 2001. Pax6 is required for the multipotent state of retinal progenitor cells. Cell 105, 43-55, http://www.ncbi.nlm.nih.gov/pubmed/11301001
Matter-Sadzinski, L., Puzianowska-Kuznicka, M., Hernandez, J., Ballivet, M., Matter, J.M., 2005. A bHLH transcriptional network regulating the specification of retinal ganglion cells. Development 132, 3907-3921, 10.1242/dev.01960.

Maurer, K.A., Riesenberg, A.N., Brown, N.L., 2014. Notch signaling differentially regulates Atoh7 and Neurog2 in the distal mouse retina. Development 141, 3243-3254, 10.1242/dev.106245.
Mersfelder, E.L., Parthun, M.R., 2006. The tale beyond the tail: histone core domain modifications and the regulation of chromatin structure. Nucleic Acids Res 34, 2653-2662, 10.1093/nar/gkl338.
Mu, X., Fu, X., Beremand, P.D., Thomas, T.L., Klein, W.H., 2008. Gene regulation logic in retinal ganglion cell development: Isl1 defines a critical branch distinct from but overlapping with Pou4f2. Proceedings of the National Academy of Sciences of the United States of America 105, 6942-6947, 10.1073/pnas.0802627105.
Mu, X., Fu, X., Sun, H., Beremand, P.D., Thomas, T.L., Klein, W.H., 2005. A gene network downstream of transcription factor Math5 regulates retinal progenitor cell competence and ganglion cell fate. Developmental biology 280, 467-481, 10.1016/j.ydbio.2005.01.028.
Otteson, D.C., D'Costa, A.R., Hitchcock, P.F., 2001. Putative stem cells and the lineage of rod photoreceptors in the mature retina of the goldfish. Developmental biology 232, 62-76, 10.1006/dbio.2001.0163.
Otteson, D.C., Phillips, M.J., 2010. A conditional immortalized mouse muller glial cell line expressing glial and retinal stem cell genes. Invest. Ophthalmol. Vis. Sci. 51, 5991-6000, 10.1167/iovs.10-5395.
Otteson, D.C., Shelden, E., Jones, J.M., Kameoka, J., Hitchcock, P.F., 1998. Pax2 expression and retinal morphogenesis in the normal and Krd mouse. Developmental biology 193, 209-224, 10.1006/dbio.1997.8794.
Pan, L., Yang, Z., Feng, L., Gan, L., 2005. Functional equivalence of Brn3 POU-domain transcription factors in mouse retinal neurogenesis. Development 132, 703-712, 10.1242/dev.01646.
Park, J.Y., Juhnn, Y.S., 2017. cAMP signaling increases histone deacetylase 8 expression via the Epac2-Rap1A-Akt pathway in H1299 lung cancer cells. Exp. Mol. Med. 49, e297, 10.1038/emm.2016.152.
Pfaffl, M.W., Horgan, G.W., Dempfle, L., 2002. Relative expression software tool (REST) for group-wise comparison and statistical analysis of relative expression results in real-time PCR. Nucleic Acids Res. 30, e36, http://www.ncbi.nlm.nih.gov/pubmed/11972351
Phillips, M.J., Perez, E.T., Martin, J.M., Reshel, S.T., Wallace, K.A., Capowski, E.E., Singh, R., Wright, L.S., Clark, E.M., Barney, P.M., Stewart, R., Dickerson, S.J., Miller, M.J., Percin, E.F., Thomson, J.A., Gamm, D.M., 2014. Modeling human retinal development with patient-specific induced pluripotent stem cells reveals multiple roles for visual system homeobox 2. Stem Cells 32, 1480-1492, 10.1002/stem.1667.
Qiao, Y., Wang, R., Yang, X., Tang, K., Jing, N., 2015. Dual roles of histone H3 lysine 9 acetylation in human embryonic stem cell pluripotency and neural differentiation. The Journal of biological chemistry 290, 2508-2520, 10.1074/jbc.M114.603761.
Raj, A., Peskin, C.S., Tranchina, D., Vargas, D.Y., Tyagi, S., 2006. Stochastic mRNA synthesis in mammalian cells. PLoS Biol. 4, e309, 10.1371/journal.pbio.0040309.
Reichert, N., Choukrallah, M.A., Matthias, P., 2012. Multiple roles of class I HDACs in proliferation, differentiation, and development. Cell Mol Life Sci 69, 2173-2187, 10.1007/s00018-012-0921-9.
Riesenberg, A.N., Liu, Z., Kopan, R., Brown, N.L., 2009. Rbpj cell autonomous regulation of retinal ganglion cell and cone photoreceptor fates in the mouse retina. The Journal of neuroscience : the official journal of the Society for Neuroscience 29, 12865-12877, 10.1523/JNEUROSCI.3382-09.2009.
Rousseaux, S., Khochbin, S., 2015. Histone Acylation beyond Acetylation: Terra Incognita in Chromatin Biology. Cell J 17, 1-6, http://www.ncbi.nlm.nih.gov/pubmed/25870829
Saunders, A., Huang, X., Fidalgo, M., Reimer, M.H., Jr., Faiola, F., Ding, J., Sanchez-Priego, C., Guallar, D., Saenz, C., Li, D., Wang, J., 2017. The SIN3A/HDAC Corepressor Complex Functionally Cooperates with NANOG to Promote Pluripotency. Cell reports 18, 1713-1726, 10.1016/j.celrep.2017.01.055.
Schmalenberger, B., 1980. Differentiation of the guinea pig eye: nuclear ultrastructure, template activity and DNA content. Protoplasma 103, 377-391, http://www.ncbi.nlm.nih.gov/pubmed/6158745

Schubert, T., Huckfeldt, R.M., Parker, E., Campbell, J.E., Wong, R.O., 2010. Assembly of the outer retina in the absence of GABA synthesis in horizontal cells. Neural Dev 5, 15, 10.1186/1749-8104-5-15.
Segre, C.V., Chiocca, S., 2011. Regulating the regulators: the post-translational code of class I HDAC1 and HDAC2. J Biomed Biotechnol 2011, 690848, 10.1155/2011/690848.
Seto, E., Yoshida, M., 2014. Erasers of histone acetylation: the histone deacetylase enzymes. Cold Spring Harb. Perspect. Biol. 6, a018713, 10.1101/cshperspect.a018713.
Shaked, M., Weissmuller, K., Svoboda, H., Hortschansky, P., Nishino, N., Wolfl, S., Tucker, K.L., 2008. Histone deacetylases control neurogenesis in embryonic brain by inhibition of BMP2/4 signaling. PLoS One 3, e2668, 10.1371/journal.pone.0002668.
Solovei, I., Kreysing, M., Lanctot, C., Kosem, S., Peichl, L., Cremer, T., Guck, J., Joffe, B., 2009. Nuclear architecture of rod photoreceptor cells adapts to vision in mammalian evolution. Cell 137, 356-368, 10.1016/j.cell.2009.01.052.
Solovei, I., Thanisch, K., Feodorova, Y., 2016. How to rule the nucleus: divide et impera. Curr Opin Cell Biol 40, 47-59, 10.1016/j.ceb.2016.02.014.
Song, C., Feodorova, Y., Guy, J., Peichl, L., Jost, K.L., Kimura, H., Cardoso, M.C., Bird, A., Leonhardt, H., Joffe, B., Solovei, I., 2014. DNA methylation reader MECP2: cell type- and differentiation stage-specific protein distribution. Epigenetics Chromatin 7, 17, 10.1186/1756-8935-7-17.
Stadler, J.A., Shkumatava, A., Norton, W.H., Rau, M.J., Geisler, R., Fischer, S., Neumann, C.J., 2005. Histone deacetylase 1 is required for cell cycle exit and differentiation in the zebrafish retina. Dev Dyn 233, 883-889, 10.1002/dvdy.20427.
Staszkiewicz, J., Power, R.A., Harkins, L.L., Barnes, C.W., Strickler, K.L., Rim, J.S., Bondioli, K.R., Eilersten, K.J., 2013. Silencing histone deacetylase-specific isoforms enhances expression of pluripotency genes in bovine fibroblasts. Cell Reprogram 15, 397-404, 10.1089/cell.2013.0026.
Takase, K., Oda, S., Kuroda, M., Funato, H., 2013. Monoaminergic and neuropeptidergic neurons have distinct expression profiles of histone deacetylases. PLoS One 8, e58473, 10.1371/journal.pone.0058473.
Taniguchi, Y., Choi, P.J., Li, G.W., Chen, H., Babu, M., Hearn, J., Emili, A., Xie, X.S., 2010. Quantifying E. coli proteome and transcriptome with single-molecule sensitivity in single cells. Science 329, 533-538, 10.1126/science.1188308.
Taranova, O.V., Magness, S.T., Fagan, B.M., Wu, Y., Surzenko, N., Hutton, S.R., Pevny, L.H., 2006. SOX2 is a dose-dependent regulator of retinal neural progenitor competence. Genes Dev. 20, 1187-1202, 10.1101/gad.1407906.
Tetreault, N., Champagne, M.P., Bernier, G., 2009. The LIM homeobox transcription factor Lhx2 is required to specify the retina field and synergistically cooperates with Pax6 for Six6 trans-activation. Dev. Biol. 327, 541-550, 10.1016/j.ydbio.2008.12.022.
Thomas, E.A., 2014. Involvement of HDAC1 and HDAC3 in the Pathology of Polyglutamine Disorders: Therapeutic Implications for Selective HDAC1/HDAC3 Inhibitors. Pharmaceuticals (Basel) 7, 634-661, 10.3390/ph7060634.
Tiwari, S., Dharmarajan, S., Shivanna, M., Otteson, D.C., Belecky-Adams, T.L., 2014. Histone deacetylase expression patterns in developing murine optic nerve. BMC Dev. Biol. 14, 30, 10.1186/1471-213X-14-30.
Van Bortle, K., Corces, V.G., 2013. The role of chromatin insulators in nuclear architecture and genome function. Curr Opin Genet Dev 23, 212-218, 10.1016/j.gde.2012.11.003.
Vihtelic, T.S., Hyde, D.R., 2000. Light-induced rod and cone cell death and regeneration in the adult albino zebrafish (Danio rerio) retina. J Neurobiol 44, 289-307, http://www.ncbi.nlm.nih.gov/pubmed/10942883
Wallace, D.M., Donovan, M., Cotter, T.G., 2006. Histone deacetylase activity regulates apaf-1 and caspase 3 expression in the developing mouse retina. Investigative ophthalmology & visual science 47, 2765-2772, 10.1167/iovs.05-1383.

Waltregny, D., De Leval, L., Glenisson, W., Ly Tran, S., North, B.J., Bellahcene, A., Weidle, U., Verdin, E., Castronovo, V., 2004. Expression of histone deacetylase 8, a class I histone deacetylase, is restricted to cells showing smooth muscle differentiation in normal human tissues. Am. J. Pathol. 165, 553-564, 10.1016/S0002-9440(10)63320-2.
Wang, H., Luo, Y., Lin, Z., Lee, I.W., Kwon, J., Cui, X.S., Kim, N.H., 2015. Effect of ATM and HDAC Inhibition on Etoposide-Induced DNA Damage in Porcine Early Preimplantation Embryos. PloS one 10, e0142561, 10.1371/journal.pone.0142561.
Wang, S.W., Kim, B.S., Ding, K., Wang, H., Sun, D., Johnson, R.L., Klein, W.H., Gan, L., 2001. Requirement for math5 in the development of retinal ganglion cells. Genes Dev. 15, 24-29, http://www.ncbi.nlm.nih.gov/pubmed/11156601
Wilting, R.H., Yanover, E., Heideman, M.R., Jacobs, H., Horner, J., van der Torre, J., DePinho, R.A., Dannenberg, J.H., 2010. Overlapping functions of Hdac1 and Hdac2 in cell cycle regulation and haematopoiesis. EMBO J 29, 2586-2597, 10.1038/emboj.2010.136.
Wong, L.L., Rapaport, D.H., 2009. Defining retinal progenitor cell competence in Xenopus laevis by clonal analysis. Development 136, 1707-1715, 10.1242/dev.027607.
Yamaguchi, M., Tonou-Fujimori, N., Komori, A., Maeda, R., Nojima, Y., Li, H., Okamoto, H., Masai, I., 2005. Histone deacetylase 1 regulates retinal neurogenesis in zebrafish by suppressing Wnt and Notch signaling pathways. Development 132, 3027-3043, http://www.ncbi.nlm.nih.gov/entrez/query.fcgi?cmd=Retrieve&db=PubMed&dopt=Citation&list_uids=15944187
Yang, Z., Ding, K., Pan, L., Deng, M., Gan, L., 2003. Math5 determines the competence state of retinal ganglion cell progenitors. Developmental biology 264, 240-254, http://www.ncbi.nlm.nih.gov/pubmed/14623245
Yano, M., Yasuda, M., Sakaki, M., Nagata, K., Fujino, T., Arai, E., Hasebe, T., Miyazawa, M., Miyazawa, M., Ogane, N., Hasegawa, K., Narahara, H., 2018. Association of histone deacetylase expression with histology and prognosis of ovarian cancer. Oncol. Lett. 15, 3524-3531, 10.3892/ol.2018.7726.
Yao, K., Qiu, S., Wang, Y.V., Park, S.J.H., Mohns, E.J., Mehta, B., Liu, X., Chang, B., Zenisek, D., Crair, M.C., Demb, J.B., Chen, B., 2018. Restoration of vision after de novo genesis of rod photoreceptors in mammalian retinas. Nature 560, 484-488, 10.1038/s41586-018-0425-3.
Yao, Y.L., Yang, W.M., 2011. Beyond histone and deacetylase: an overview of cytoplasmic histone deacetylases and their nonhistone substrates. J Biomed Biotechnol 2011, 146493, 10.1155/2011/146493.
Young, R.W., 1985. Cell differentiation in the retina of the mouse. Anat. Rec. 212, 199-205, 10.1002/ar.1092120215.
Zahnow, C.A., Topper, M., Stone, M., Murray-Stewart, T., Li, H., Baylin, S.B., Casero, R.A., Jr., 2016. Inhibitors of DNA Methylation, Histone Deacetylation, and Histone Demethylation: A Perfect Combination for Cancer Therapy. Adv. Cancer Res. 130, 55-111, 10.1016/bs.acr.2016.01.007.
Zhang, Y., Stone, J., 1997. Role of astrocytes in the control of developing retinal vessels. Invest. Ophthalmol. Vis. Sci. 38, 1653-1666, http://www.ncbi.nlm.nih.gov/entrez/query.fcgi?cmd=Retrieve&db=PubMed&dopt=Citation&list_uids=9286254
Zhou, Q., Dalgard, C.L., Wynder, C., Doughty, M.L., 2011. Histone deacetylase inhibitors SAHA and sodium butyrate block G1-to-S cell cycle progression in neurosphere formation by adult subventricular cells. BMC Neurosci 12, 50, 10.1186/1471-2202-12-50.
Zuber, M.E., Gestri, G., Viczian, A.S., Barsacchi, G., Harris, W.A., 2003. Specification of the vertebrate eye by a network of eye field transcription factors. Development 130, 5155-5167, 10.1242/dev.00723.

Table 1: Change in nuclear localization between NPC and RGCs at the same stage

HDAC	E16		P5	
	NPCs SOX2	GCs POU4F	NPCs SOX2	GCs POU4F
HDAC1	**+**	**++**	**-**	**+**
HDAC2	**-**	**+/-**	**-**	**++**
HDAC3	**+/-**	**+/-**	**+/-**	**++**
HDAC8	**-**	**+**	**-**	**+**

NPCs; neural progenitor cells, GCs; ganglion cells
+ weak nuclear colocalization, ++ strong nuclear colocalization, +/- mixed nuclear colocalization, - no nuclear colocalization

Table 2: Localization of classical HDACs in nuclei of retinal cell types

HDAC	AMs (SOX2)		Astros (SOX2)		GCs (POU4F)		MGs (SOX2)
	P5	P30	P5	P30	P5	P30	P30
HDAC1	+	++	+	++	+	++	+
HDAC2	++	+	++	++	+	++	-
HDAC3	+	+	+	++	++	++	-
HDAC8	+	-	+	-	+	-	-

GCs; ganglion cells, AMs; amacrine cells, Astros; astrocytes, PhRs; photoreceptors, MGs; Müller Glia

+ weak colocalization, ++ strong colocalization, +/- mixed colocalization, - no colocalization

Blue- no or slight change

Green expression levels went up

Red-expression levels went down

Antibody	Source	Antibody Dilution		Peptide Supplier
		IHC	Westerns	
Rabbit Anti-HDAC1 (Cat# LS-B6094, **RRID:AB_10944903)**	Life Span Biosciences (Seattle, WA)	1:200	1:2500	Abcam (Cambridge, MA)
Mouse Anti-HDAC2 (Cat# ab12169, **RRID:AB_2118547**)	ABCAM (Cambridge, MA)	1:350	1:2500	Abcam (Cambridge, MA)
Rabbit Anti-HDAC3 (Cat#3949, **RRID:AB_2118371**)	Cell Signaling (Danvers, MA)	1:300	1:2500	Abcam (Cambridge, MA)
Rabbit Anti-HDAC8 (Cat# LS-B967, **RRID:AB_2116942**)	Life Span Biosciences (Seattle, WA)	1:300	1:1000	Life Span Biosciences
Mouse anti-BRN3A (**Millipore Cat# MAB1585, RRID:AB_94166**)	Millipore	1:100 1:500 (tyr)	N/A	N/A
Rabbit anti-BRN3A (Cat#ab81213; **RRID:AB_1640222)**	Abcam (Cambridge, MA)	1:100	N/A	N/A
Goat anti-BRN3C (Cat# sc-6026, **RRID:AB_673441**)	Santa cruz	1:100	N/A	N/A
Mouse Anti-methylated histone (Cat# ab1220, **RRID:AB_449854**)	ABCAM (Cambridge, MA)	1:1000 (tyr)	N/A	N/A
Rabbit Anti-Acetylated histone H3 K9 (Cat# ab12179, **RRID:AB_298910**)	Cell Signaling (Danvers, MA)	1:100	1:2000	N/A
Goat Anti-SOX2 (Cat# sc17320, **RRID:AB_2286684**)	Santa Cruz (Santa Cruz, CA)	1:250	N/A	Santa Cruz (Santa Cruz, CA)
Mouse Anti SOX2 (Cat# ab75485, **RRID:AB_1278243)**	ABCAM (Cambridge, MA)	1:100	N/A	Abcam (Cambridge, MA))
Mouse anti-β-tubulin (Cat# T0198, **RRID:AB_477556**)	SIGMA (St. Louis, MO)	N/A	1:1000	N/A

Table 3: Key Resources Table

tyr; used with tyramide amplification, N/A, not applicable

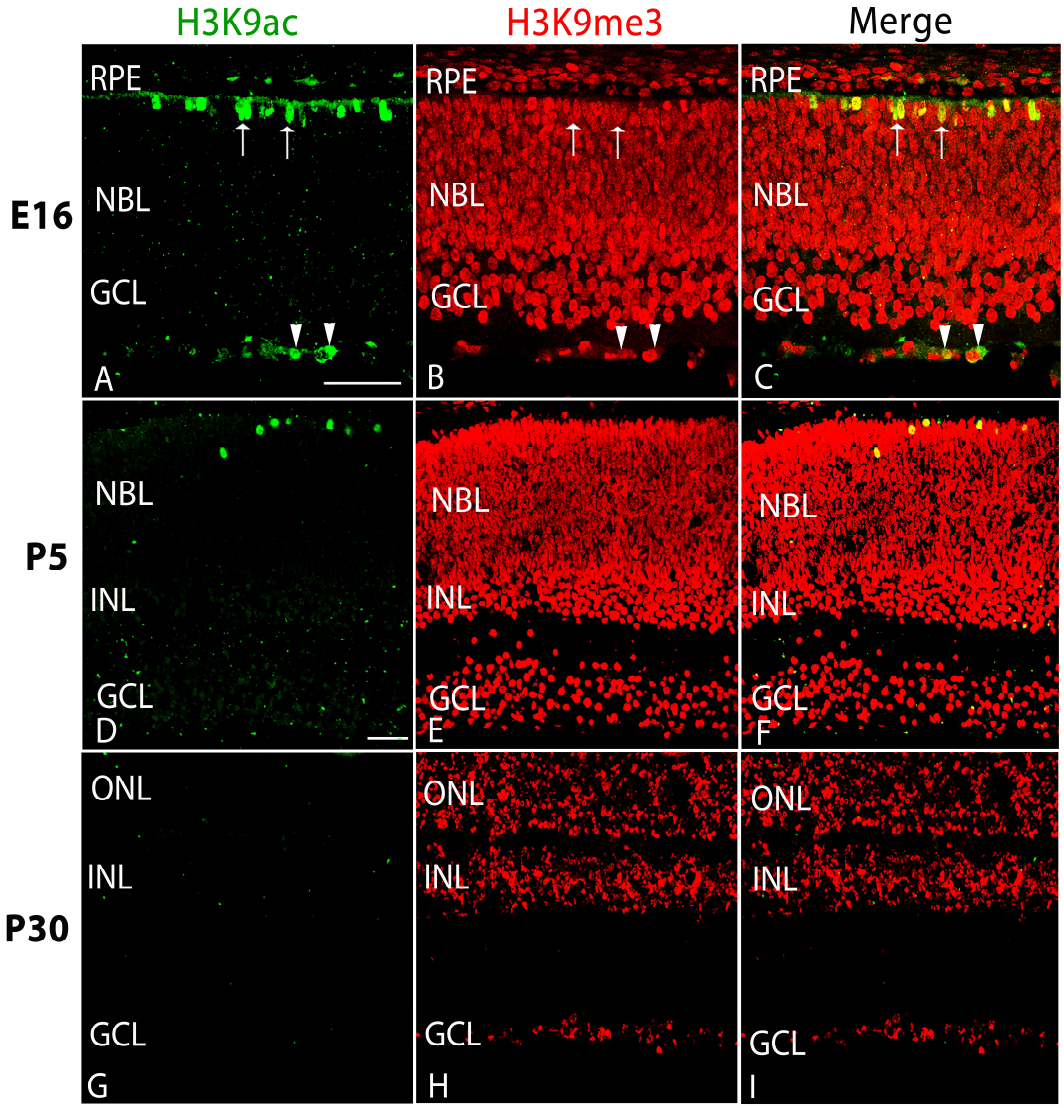

Figure 1 Localization of acetyled H3K9 (H3K9ac) and tri-methylated H3K9 (H3K9me3) in murine retina

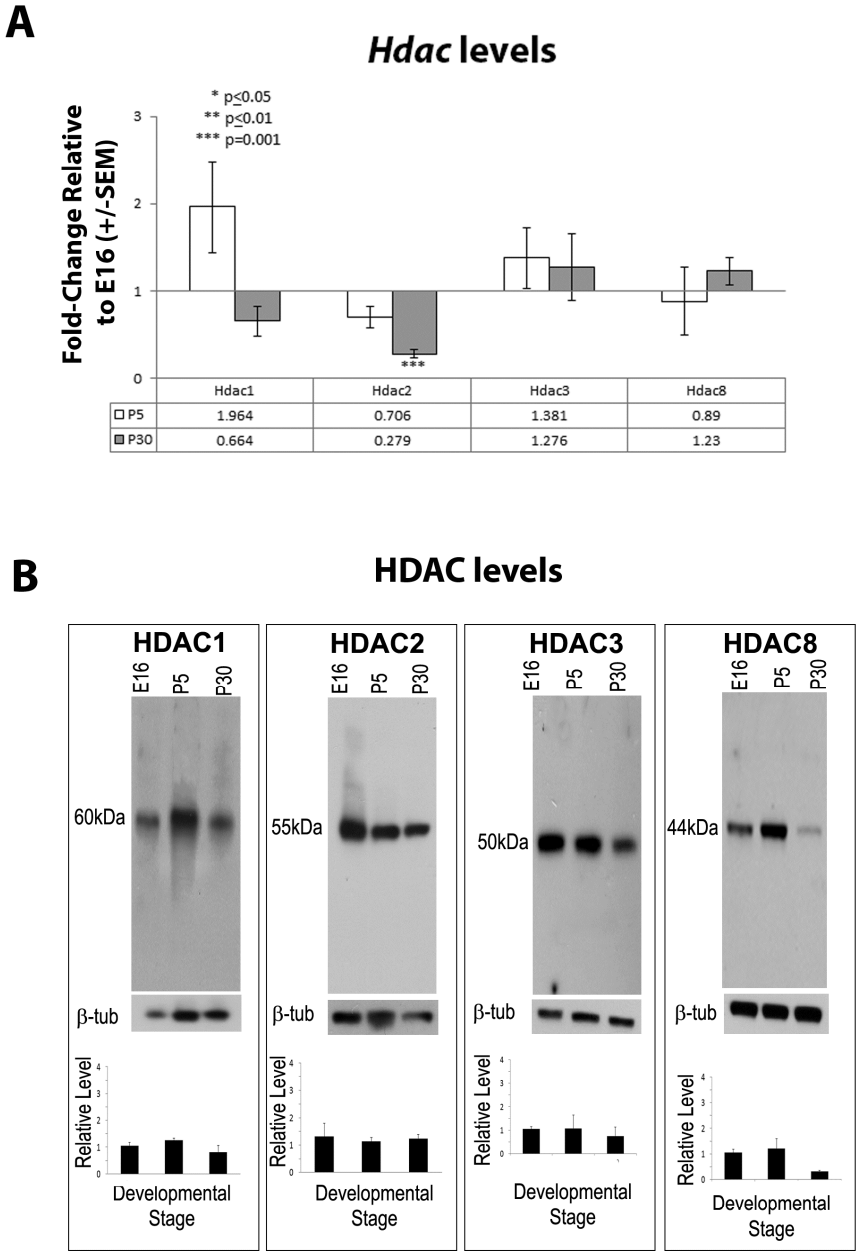

Figure 2 Analyses of mRNA and protein levels in murine retina

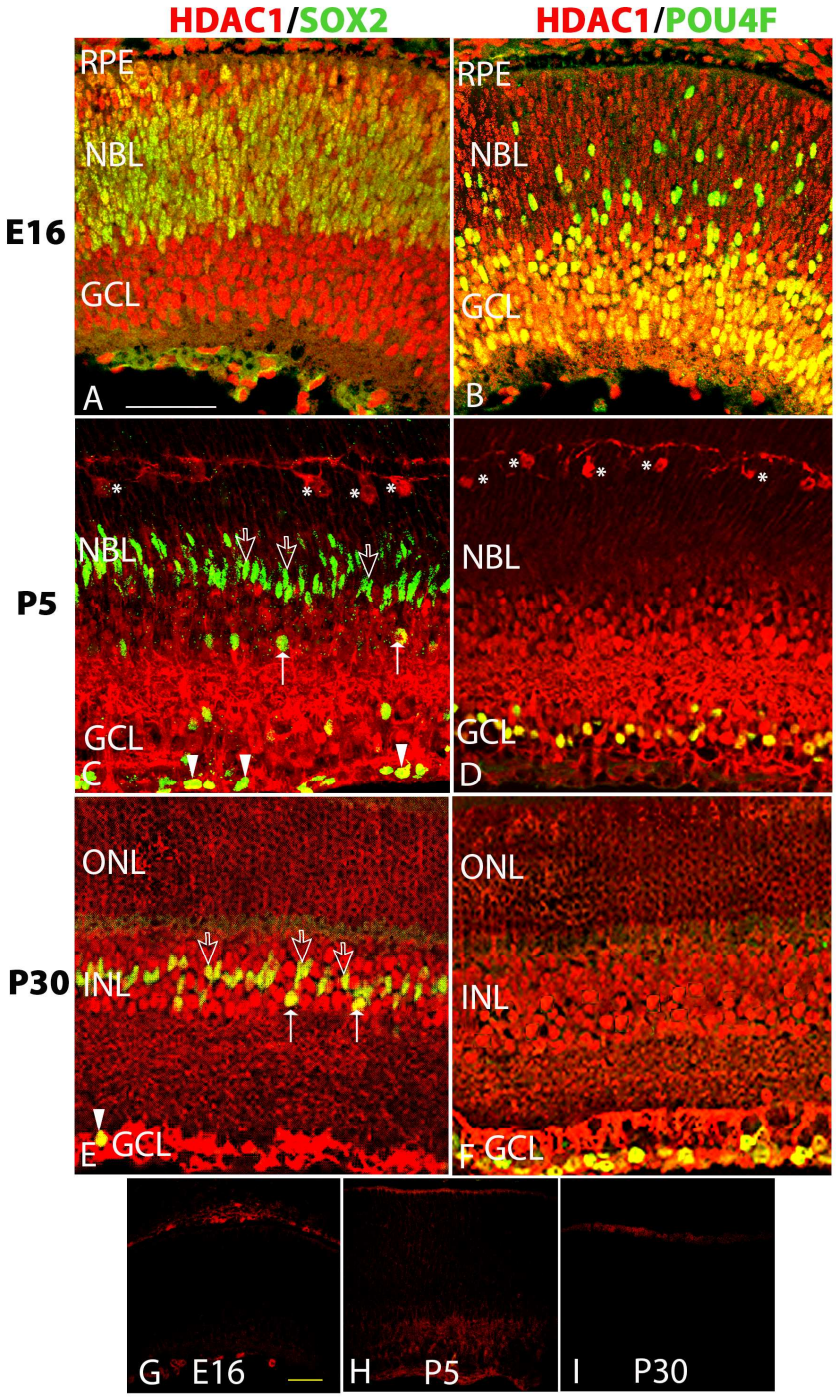

Figure 3 HDAC1 Localization in developing murine retina

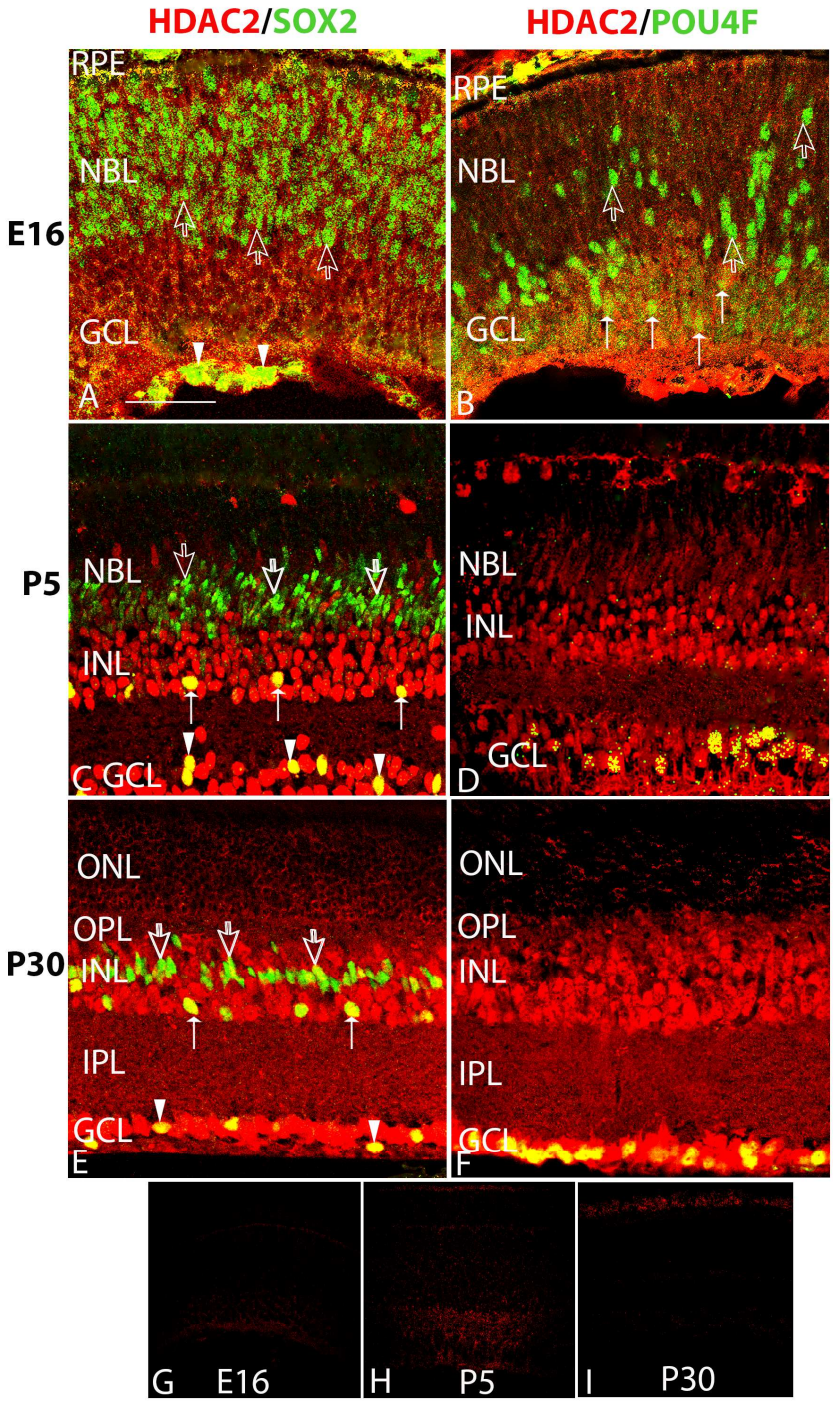

Figure 4 HDAC2 Localization in developing murine retina

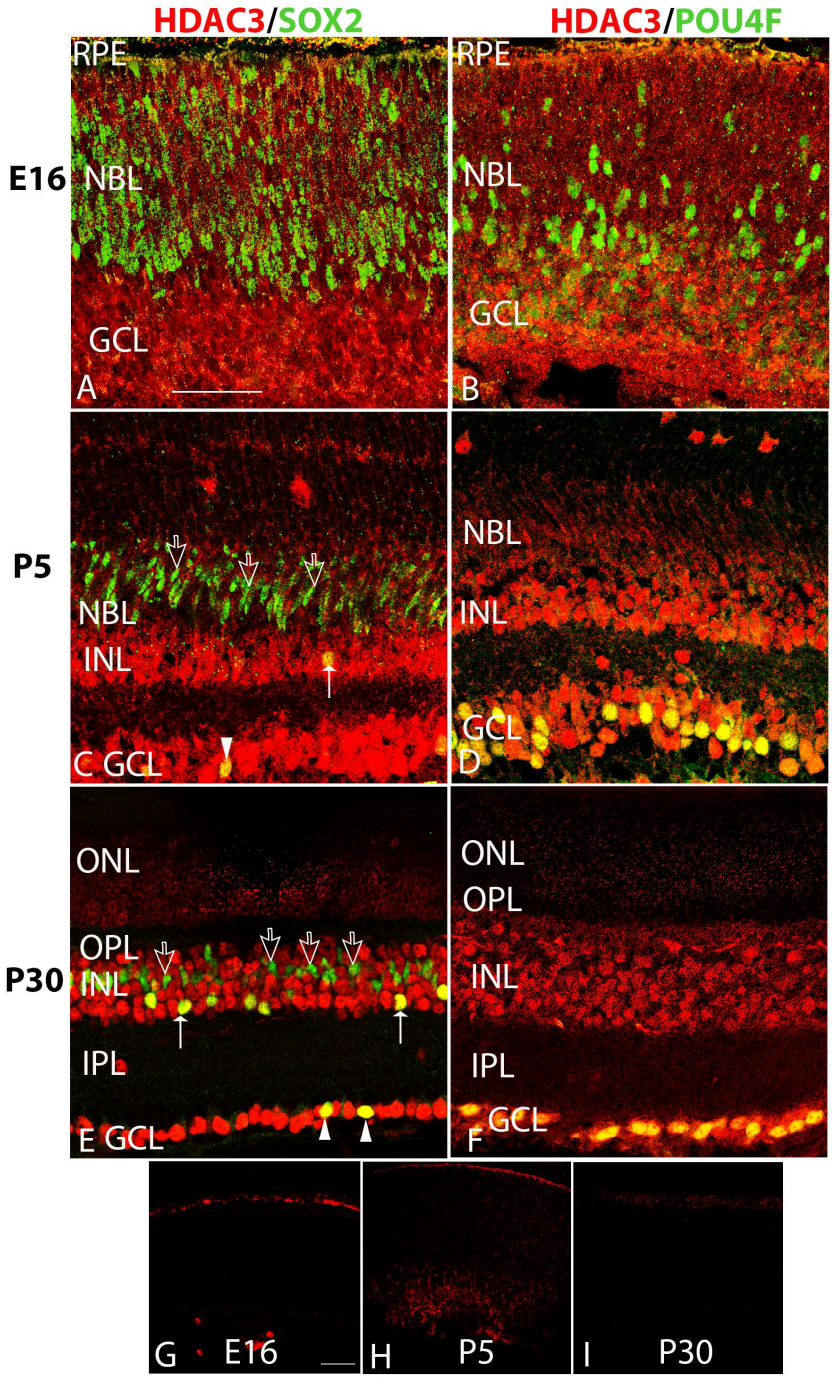

Figure 5 HDAC3 Localization in developing murine retina

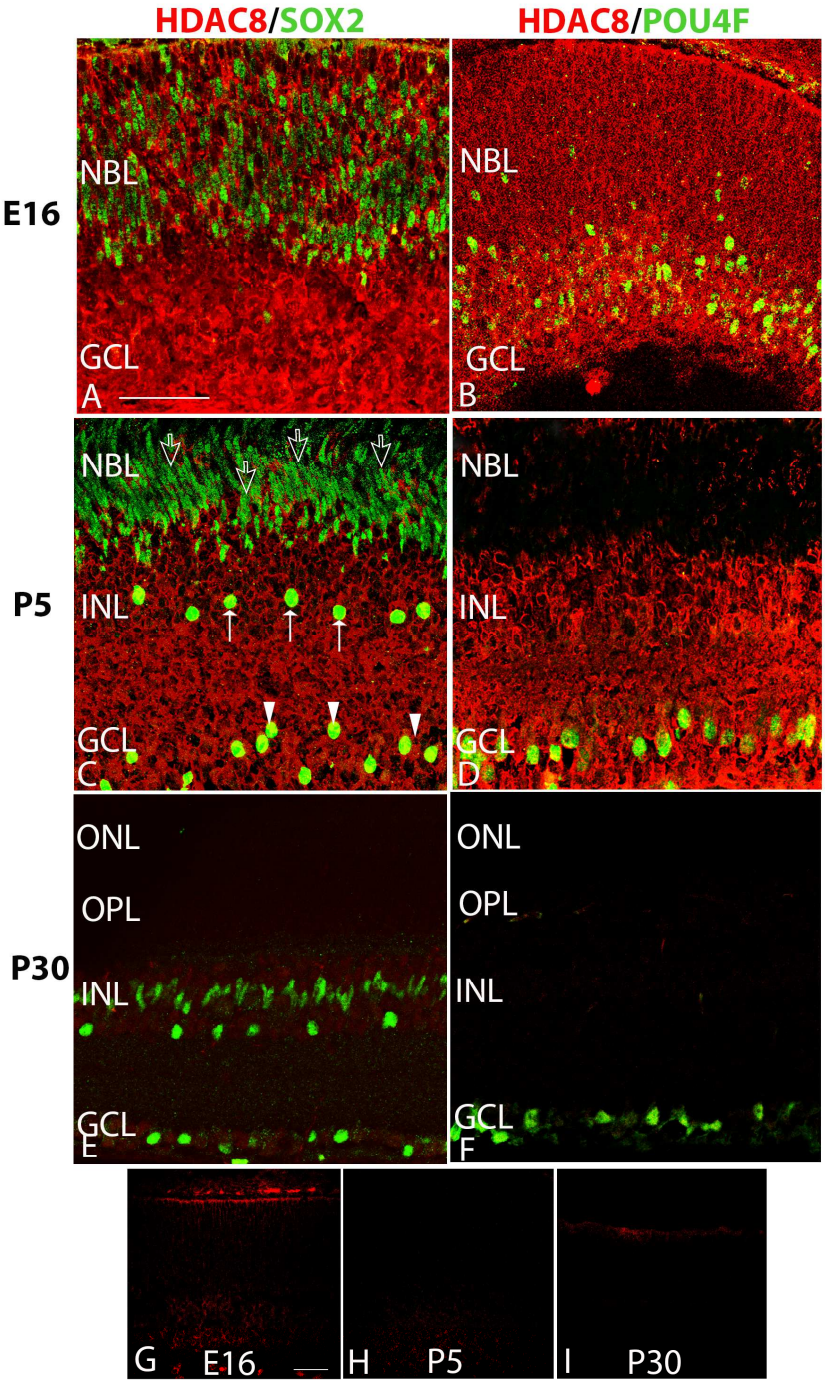

Figure 6 HDAC8 Localization in developing murine retina

Highlights

- Dynamic changes in subcellular localization of Class I HDACs was observed, despite relatively minor changes in levels of mRNA or protein
- Very few retinal progenitors were positive for acetylated H3K9, a marker of open chromatin and active gene transcription, whereas most retinal progenitors were positive for tri-methylated H3K9.
- HDAC1 was the only Class I HDAC localized to the nucleus of retinal progenitors and differentiated retinal ganglion cells
- HDACs 2 and 3 were not detected in retinal progenitor nuclei, but were present in inner nuclear layer and ganglion cell layer nuclei.
- Class I HDACs may play significant roles in the chromatin reorganization that occurs during the differentiation of mammalian retinal neurons and glia.